

Excitation of Disk Oscillations by Warps: A Model of kHz QPOs

Shoji KATO

Department of Informatics, Nara Sangyo University, Ikoma-gun, Nara 636-8503

kato@io.nara-su.ac.jp; kato@kusastro.kyoto-u.ac.jp

(Received 2004 May 5; accepted 2004 July 2)

Abstract

The amplification of disk oscillations resulting from non-linear resonant couplings between the oscillations and a warp is examined. The disks are geometrically thin and general relativistic with non-rotating central objects. By using a Lagrangian formulation, a general stability criterion is derived. The criterion is applied to horizontal and vertical resonances of g-mode oscillations and to horizontal resonances of p-mode oscillations. The results of analyses show that g-mode oscillations (including p-mode oscillations of $n = 0$) are amplified by horizontal resonances with the warp. Other modes of oscillations with other resonances are all damped by resonances. The amplified g-mode oscillations are located around the radius $4r_g$, the radius of the epicyclic frequency being maximum, i.e., κ_{\max} . The frequencies of amplified oscillations are harmonics of κ_{\max} , and well explain the 2 : 3 pairs of observed QPOs for reasonable masses (and spins) of the central objects.

Key words: accretion, accretion disks — black holes — kilohertz quasi-periodic oscillations — relativity — warps — X-rays; stars

1. Introduction

Kilohertz quasi-periodic oscillations (kHz QPOs) have been observed in many X-ray binaries. They are observed in both neutron stars and black holes (for review, e.g., van der Klis 2000). Recently, they were also observed in X-ray pulsars (Wijnands et al. 2003). One of the reasons why much attention is being paid to kHz QPOs is that they give a clue for understanding the structure of the innermost region of relativistic disks, and provide powerful information concerning the masses and spins of the central objects.

One of characteristics of kHz QPOs in black hole binaries is that they appear in pairs in many objects, and their frequency ratios are close to 2 : 3. Paying attention on these points, Abramowicz and Kluzniak (2001) and Kluzniak and Abramowicz (2001) suggested that a

parametric resonance is the cause of these QPOs. Subsequently, they and their group developed their idea in many subsequent papers (as recent papers, see, for example, Abramowicz, Kluźniak 2003; Abramowicz et al. 2004a; Abramowicz et al. 2004b). For a parametric resonance to work, disks must be deformed. A well-known example of the excitation of oscillations on deformed disks is a precession of disks deformed by a tidal force (Whitehurst 1988; Hirose, Osaki 1990; Lubow 1991). Another example is excitation of a spiral pattern in galactic disks deformed by ram-pressure (Tosa 1994; Kato, Tosa 1994). In the context of kHz QPOs, Kato (2003) considered disks deformed by a warp, and studied non-linear resonant interactions between the warp and g-mode oscillations on disks. He showed that some g-mode oscillations are amplified on the disks by resonances, and suggested that they would be the cause of QPOs.

The main purpose of this paper is to re-examine more generally and more carefully the amplification of disk oscillations resulting from resonant couplings between a warp and the oscillations, correcting some errors in Kato (2003). That is, we elaborate formulations while studying the condition of nonlinear resonant amplifications by adopting the Lagrangian formulation (Lynden-Bell, Ostriker 1967) of hydrodynamical equations. [In Kato (2003) Eulerian formulations are adopted.] There are two superior points in Lagrangian formulations. The first is that the non-linear coupling terms expressed in Cartesian coordinates are compact. The second is that the linear part of hydrodynamical equations can be expressed in terms of Hermite operators (Lynden-Bell, Ostriker 1967). This makes stability analyses perspective, and allows us to derive a general stability criterion.

As a preparation for systematically studying which resonances amplify oscillations, the types of resonant couplings between a warp and oscillations were examined in detail in a previous paper (Kato 2004, hereafter Paper I). The second purpose of this paper is to show, by calculating the growth rates, which resonances really amplify oscillations, and to suggest the origin of the observed kHz QPOs.

2. Basic Non-Linear Equations and a General Stability Criterion

An unperturbed disk is geometrically thin, non-selfgravitating, and relativistic without accretion flow. The effects of general relativity are taken into account within the framework of a pseudo-Newtonian formulation using the gravitational potential introduced by Paczyński and Wiita (1980), no rotation of the central object being assumed. This means that all calculations of non-linear coupling terms are made within the framework of the Newtonian hydrodynamics, changing only the Newtonian gravitational potential to that of Paczyński and Wiita.

2.1. *Non-linear Hydrodynamical Equations of Lagrangian Formulation*

In a Lagrangian formulation, the hydrodynamical equation describing perturbations can be written as (Lynden-Bell, Ostriker 1967)

$$\frac{D_0^2 \boldsymbol{\xi}}{Dt^2} = \delta \left(-\nabla \psi - \frac{1}{\rho} \nabla p \right), \quad (1)$$

where $\boldsymbol{\xi}$ is a displacement associated with perturbations, and D_0/Dt is the time derivative along an unperturbed flow, \mathbf{u}_0 , and is related to the Eulerian time derivative, $\partial/\partial t$, by

$$\frac{D_0}{Dt} = \frac{\partial}{\partial t} + \mathbf{u}_0 \cdot \nabla. \quad (2)$$

In equation (1), δ represents the Lagrangian variation of the quantities in the subsequent parentheses, and ψ is the gravitational potential. Other notations in equation (1) have their usual meanings.

The Lagrangian change of a quantity, $Q(\mathbf{r}, t)$, i.e., δQ , is defined by

$$\delta Q = Q[\mathbf{r} + \boldsymbol{\xi}(\mathbf{r}, t)] - Q_0(\mathbf{r}, t), \quad (3)$$

where the subscript 0 to Q represents the unperturbed value. The Eulerian change of Q , i.e., Q_1 , on the other hand, is defined by

$$Q_1 = Q(\mathbf{r}, t) - Q_0(\mathbf{r}, t). \quad (4)$$

If $Q[\mathbf{r} + \boldsymbol{\xi}(\mathbf{r}, t), t]$ is Taylor-expanded around $Q(\mathbf{r})$ up to the second-order terms with respect to perturbations, we have, from equations (3) and (4),

$$\delta Q = Q_1 + \xi_j \frac{\partial Q_0}{\partial r_j} + \xi_j \frac{\partial Q_1}{\partial r_j} + \frac{1}{2} \xi_i \xi_j \frac{\partial^2 Q_0}{\partial r_i \partial r_j}. \quad (5)$$

This is a relation between δQ and Q_1 , up to the second-order small quantities with respect to perturbations. Here and hereafter, subscripts 0 and 1 are used to represent the unperturbed and (Eulerian) perturbed quantities, respectively. Furthermore, here and hereafter, the summation abbreviation is adopted, using Cartesian coordinates. (In the final calculations of the growth rate of the resonance interactions we adopt cylindrical coordinates.)

Our purpose here is to explicitly write down equation (1) up to the second-order small quantities with respect to perturbations. Since the self-gravity of the disk is neglected here, i.e., $\psi_1 = 0$, we have easily

$$\delta(\nabla \psi) = \xi_j \frac{\partial}{\partial r_j} (\nabla \psi_0) + \frac{1}{2} \xi_i \xi_j \frac{\partial^2}{\partial r_i \partial r_j} (\nabla \psi_0). \quad (6)$$

The second term on the right-hand side of equation (6) represents non-linear terms. Expressing $\delta(\nabla p/\rho)$ in terms of Lagrangian quantities is, on the other hand, somewhat complicated. Using equation (5) and the definition of Lagrangian change, we have

$$\begin{aligned} \delta \left(\frac{1}{\rho} \nabla p \right) &= \frac{1}{\rho_0 + \delta \rho} \left[\nabla p_0 + \nabla p_1 + \xi_j \frac{\partial}{\partial r_j} \nabla (p_0 + p_1) \right. \\ &\quad \left. + \frac{1}{2} \xi_i \xi_j \frac{\partial^2}{\partial r_i \partial r_j} \nabla p_0 + \dots \right] - \frac{1}{\rho_0} \nabla p_0. \end{aligned} \quad (7)$$

The Eulerian pressure variation, p_1 , which appears on the right-hand side of equation (7), is expressed in terms of δp and $\boldsymbol{\xi}$ by using

$$\delta p = p_1 + \xi_j \frac{\partial}{\partial r_j} (p_0 + p_1) + \frac{1}{2} \xi_i \xi_j \frac{\partial^2 p_0}{\partial r_i \partial r_j}. \quad (8)$$

We then have

$$\begin{aligned} \rho_0 \delta \left(\frac{1}{\rho} \nabla p \right) = & \nabla \left[\delta p - \xi_j \frac{\partial p_0}{\partial r_j} - \xi_j \frac{\partial}{\partial r_j} \left(\delta p - \xi_i \frac{\partial p_0}{\partial r_i} \right) - \frac{1}{2} \xi_i \xi_j \frac{\partial^2 p_0}{\partial r_i \partial r_j} \right] \\ & + \xi_j \frac{\partial}{\partial r_j} \nabla \left[p_0 + \delta p - \xi_i \frac{\partial p_0}{\partial r_i} \right] + \frac{1}{2} \xi_i \xi_j \frac{\partial^2}{\partial r_i \partial r_j} \nabla p_0 \\ & - \frac{\delta \rho}{\rho_0} \left[\nabla p_0 + \nabla (\delta p) - (\nabla \xi_j) \frac{\partial p_0}{\partial r_j} \right] + \left(\frac{\delta \rho}{\rho_0} \right)^2 \nabla p_0. \end{aligned} \quad (9)$$

This explicitly expresses $\rho_0 \delta(\nabla p/\rho)$ up to the second-order quantities in terms of Lagrangian quantities, δp , $\delta \rho$, and ξ .

Next, δp and $\delta \rho$ on the right-hand side of equation (9) are explicitly expressed in terms of ξ . To do so we use the equation of continuity and the adiabatic relation. The former relation is expressed as (e.g., Kato, Unno 1967)

$$\delta \rho + \rho_0 \frac{\partial \xi_i}{\partial r_i} = \rho_0 N_c, \quad (10)$$

where

$$N_c = \frac{1}{2} \left[\left(\frac{\partial \xi_j}{\partial r_j} \right)^2 + \frac{\partial \xi_i}{\partial r_j} \frac{\partial \xi_j}{\partial r_i} \right]. \quad (11)$$

The adiabatic relation is written as (e.g., Kato, Unno 1967)

$$\frac{\delta p}{p_0} - \Gamma_1 \frac{\delta \rho}{\rho_0} = N_p, \quad (12)$$

where

$$N_p = \frac{1}{2} \Gamma_1 (\Gamma_1 - 1) \left(\frac{\delta \rho}{\rho_0} \right)^2. \quad (13)$$

Substitution of equations (10) and (12) into equation (9) finally gives an expression for $\rho_0 \delta(\nabla p/\rho)$, expressed in terms of ξ alone. This is summarized as

$$\rho_0 \delta \left(\frac{1}{\rho} \nabla p \right) = \mathbf{P}_{(1)} + \mathbf{P}_{(2)}, \quad (14)$$

where $\mathbf{P}_{(1)}$ is the linear part with respect to ξ and $\mathbf{P}_{(2)}$ is the non-linear part. An explicit form of the linear part is given by Lynden-Bell and Ostriker (1967), which is

$$\mathbf{P}_{(1)} = \nabla \left[(1 - \Gamma_1) p_0 \frac{\partial \xi_i}{\partial r_i} \right] - p_0 \nabla \left(\frac{\partial \xi_i}{\partial r_i} \right) - \nabla \left(\xi_j \frac{\partial p_0}{\partial r_j} \right) + \xi_j \frac{\partial}{\partial r_j} \nabla p_0. \quad (15)$$

The non-linear term, $\mathbf{P}_{(2)}$, generally has a complicated form. In the case of isothermal disks, i.e., $\Gamma_1 = 1$, however, it has a simple expression. We are satisfied here with using this simple expression for $\mathbf{P}_{(2)}$ in the following analyses of resonances, since the difference of Γ_1 from unity will not bring about any qualitative differences in the final results. In the case of $\Gamma_1 = 1$, after some manipulations we have

$$\mathbf{P}_{(2)} = \frac{\partial}{\partial r_i} \left(p_0 \frac{\partial \xi_i}{\partial r_j} \nabla \xi_j \right). \quad (16)$$

Hereafter, we consider time-periodic perturbations, which vary as $\exp(i\omega t)$, ω being a frequency. Then, the non-linear hydrodynamical equation for adiabatic perturbations, equation (1), is written as

$$-\omega^2 \rho_0 \boldsymbol{\xi} + 2i\omega \rho_0 (\mathbf{u}_0 \cdot \nabla) \boldsymbol{\xi} + \mathbf{L}(\boldsymbol{\xi}) = \rho_0 \mathbf{C}(\boldsymbol{\xi}, \boldsymbol{\xi}), \quad (17)$$

where \mathbf{L} is a linear operator with respect to $\boldsymbol{\xi}$, and is (Lynden-Bell, Ostriker 1967)

$$\mathbf{L}(\boldsymbol{\xi}) = \rho_0 (\mathbf{u}_0 \cdot \nabla) (\mathbf{u}_0 \cdot \nabla) \boldsymbol{\xi} + \rho_0 (\boldsymbol{\xi} \cdot \nabla) (\nabla \psi_0) + \mathbf{P}_{(1)}(\boldsymbol{\xi}). \quad (18)$$

The non-linear term $\rho_0 \mathbf{C}$ consists of two parts, i.e., $\rho_0 \mathbf{C} = \rho_0 \mathbf{C}_\psi + \rho_0 \mathbf{C}_p$, where $\rho_0 \mathbf{C}_\psi$ comes from $-\rho_0 \delta(\nabla \psi)$ and $\rho_0 \mathbf{C}_p$ from $-\rho_0 \delta(\nabla p/\rho)$. From equation (6) we have

$$\rho_0 \mathbf{C}_\psi = -\frac{1}{2} \rho_0 \xi_i \xi_j \frac{\partial^2}{\partial r_i \partial r_j} (\nabla \psi_0), \quad (19)$$

and from equation (16) we have

$$\rho_0 \mathbf{C}_p = -\frac{\partial}{\partial r_i} \left(p_0 \frac{\partial \xi_i}{\partial r_j} \nabla \xi_j \right). \quad (20)$$

Detailed expressions for $\rho_0 \mathbf{C}_\psi$ and $\rho_0 \mathbf{C}_p$ in cylindrical coordinates are given in appendix 1.

An important characteristics of the linear operator \mathbf{L} is that it is a Hermitian (Lynden-Bell, Ostriker 1967). This characteristics of \mathbf{L} is used later when we evaluate the growth rate of oscillations.

2.2. A General Method for Deriving Stability Criterion

We assume that a mode of oscillations is present on the disk with a small amplitude. The displacement associated with the oscillations is denoted by $\boldsymbol{\xi}$, which satisfies the homogeneous part of the wave equation (17). Now, we further assume that the unperturbed disk is deformed by some external forces from an equilibrium state. The displacement associated with the deformations is denoted by $\boldsymbol{\xi}^w$. Nonlinear couplings between $\boldsymbol{\xi}$ and $\boldsymbol{\xi}^w$ are now examined, assuming that they are weak and their effects can be studied by applying successive approximations. The processes of the couplings are shown schematically in figure 1. The first step of nonlinear couplings between $\boldsymbol{\xi}$ and $\boldsymbol{\xi}^w$ is their direct interactions. The resulting oscillations are denoted by $\boldsymbol{\xi}^{\text{int}}$, and hereafter called intermediate oscillations. Since we are interested here in the case when the time scale associated with the deformation is sufficiently long compared with $1/\omega$, the intermediate oscillations are described by using the inhomogeneous wave equation (17) as

$$-\omega^2 \rho_0 \boldsymbol{\xi}^{\text{int}} + 2i\omega \rho_0 (\mathbf{u}_0 \cdot \nabla) \boldsymbol{\xi}^{\text{int}} + \mathbf{L}(\boldsymbol{\xi}^{\text{int}}) = \rho_0 \mathbf{C}(\boldsymbol{\xi}, \boldsymbol{\xi}^w). \quad (21)$$

As the next step of nonlinear interactions, we consider interactions between the intermediate oscillations $\boldsymbol{\xi}^{\text{int}}$ and the deformations $\boldsymbol{\xi}^w$. This interaction is interesting, since it generally feedbacks to the original oscillations of $\boldsymbol{\xi}$. Unless a resonance phenomenon is involved in the

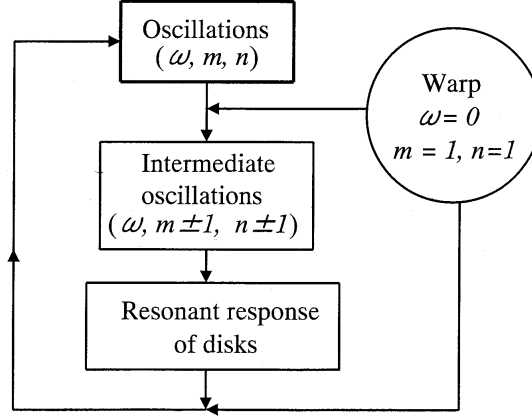


Fig. 1. Feedback processes of nonlinear resonant interactions acting on oscillations. The original oscillations are characterized by ω , m , and n . Since the warp corresponds to a wave mode of $\omega = 0$, $m = 1$, and $n = 1$, the nonlinear interaction between them brings about intermediate modes of oscillations of ω , $m \pm 1$, and $n \pm 1$. To these intermediate oscillations, the disk resonantly responds at a certain radius. Then, the intermediate oscillations feedback to the original oscillations after the resonance. This feedback process amplifies or dampens the original oscillations, since resonances are involved in the interaction processes. (After Paper I)

feedback processes, the effects of the feedbacks are only to change the frequencies and functional forms of the original oscillations. If a resonance process is involved, however, there is a possibility of the oscillations being amplified (or damped). The Lagrangian formulation of hydrodynamical equations by Lynden-Bell and Ostriker (1967) makes this analysis easy. The equation describing these feedbacks is given by

$$-\omega^2 \rho_0 \boldsymbol{\xi} + 2i\omega \rho_0 (\mathbf{u}_0 \cdot \nabla) \boldsymbol{\xi} + \mathbf{L}(\boldsymbol{\xi}) = \rho_0 \mathbf{C}(\boldsymbol{\xi}^{\text{int}}, \boldsymbol{\xi}^{\text{w}}). \quad (22)$$

That is, the left-hand side of the equation is the same as equation (17), while the coupling term is $\rho_0 \mathbf{C}(\boldsymbol{\xi}^{\text{int}}, \boldsymbol{\xi}^{\text{w}})$. Let us integrate the equation over a volume with relevant boundary conditions after multiplying by $\boldsymbol{\xi}^*$, where the asterisk denotes the complex conjugate.

Since the operators on the left-hand side of equation (22) are Hermitians, the integrations

$$i \int \rho_0 \boldsymbol{\xi}^* (\mathbf{u}_0 \cdot \nabla) \boldsymbol{\xi} dV \quad \text{and} \quad \int \boldsymbol{\xi}^* \mathbf{L}(\boldsymbol{\xi}) dV \quad (23)$$

are real. The integration of the right-hand side of the equation, on the other hand, has an imaginary part when resonances are involved in the interactions. This implies that ω must be complex. If we write $\omega = \omega_r + i\omega_i$, the imaginary part of equation (22) becomes

$$-2i\omega_i \int \boldsymbol{\xi}^* \rho_0 [\omega - i(\mathbf{u}_0 \cdot \nabla)] \boldsymbol{\xi} dV = \Im \int \rho_0 \boldsymbol{\xi}^* \mathbf{C}(\boldsymbol{\xi}^{\text{int}}, \boldsymbol{\xi}^{\text{w}}) dV. \quad (24)$$

Hereafter, ω_r is denoted by ω without any confusion. From this equation we can calculate ω_i . In the subsequent sections we examine this issue for the cases where the disk deformations are due to warps.

Equation (24) has a clear physical meaning. The integral on the left-hand side is the wave energy, E , times $2/\omega$ [see equation (92) of Kato (2001)]. Hence, the left-hand side of equation (24) represents the growing rate of the wave energy, $-2i\omega_i E$, times $2/\omega$. This implies that the right-hand side of equation (24) must be the work, W , done on the original oscillations by the force $\mathbf{C}(\boldsymbol{\xi}^{\text{int}}, \boldsymbol{\xi}^{\text{w}})$ during the time interval $2/\omega$. In other words, the work done on the oscillations by resonances, W , during a unit time is

$$W = \frac{\omega}{2} \Im \int \boldsymbol{\xi}^* \mathbf{C}(\boldsymbol{\xi}^{\text{int}}, \boldsymbol{\xi}^{\text{w}}) dV. \quad (25)$$

This is understandable, since if the velocity associated with the oscillations and the force, \mathbf{C} , are in phase as an idealized situation, the work done on the oscillations during which the displacement becomes $\boldsymbol{\xi}$ (the quarter of one cycle) is $\Im \int \boldsymbol{\xi}^* \mathbf{C}(\boldsymbol{\xi}^{\text{int}}, \boldsymbol{\xi}^{\text{w}}) dV$. Hence, the rate of work (per unit time) is, on average, $\Im \int \boldsymbol{\xi}^* \mathbf{C}(\boldsymbol{\xi}^{\text{int}}, \boldsymbol{\xi}^{\text{w}}) dV$ times $2\omega/\pi$. It is finally noted that the wave energy, E , is expressed later in a more conventional form.

3. Warps, Oscillations, and Dispersion Relation

The unperturbed disk is assumed to have no motion except for rotation. The rotation is further assumed to be cylindrical. That is, with cylindrical coordinates (r, φ, z) whose z -axis is perpendicular to the disk plane and whose origin is at the disk center, the angular velocity of rotation, Ω , is represented as $\Omega = \Omega(r)$. When we need numerical figures, we adopt the Keplerian form for Ω , i.e., $\Omega = \Omega_K(r)$, since geometrically thin disks are considered here.

The unperturbed disk is further assumed to be isothermal in the vertical direction. In vertically isothermal disks the density is stratified as (e.g., Kato et al. 1998)

$$\rho_0(r, z) = \rho_{00}(r) \exp\left(-\frac{z^2}{2H^2(r)}\right), \quad (26)$$

where ρ_{00} is the density on the equatorial plane and the half-thickness of the disk, H , is related to the angular velocity of the Keplerian rotation, Ω_K , by

$$\Omega_K^2(r) H^2(r) = \frac{p_0}{\rho_0} = c_s^2, \quad (27)$$

where c_s is the isothermal speed of sound.

3.1. Oscillations Modes and Warps

Oscillations on disks are generally a combination of motions on the equatorial plane and those in the vertical direction. These motions are coupled in complicated ways, and cannot be treated separately. In the case of the vertically isothermal disks, however, we can approximately separate them (Okazaki et al. 1987; see also Kato et al. 1998). In order to make analyses simple, we introduce here an approximation. In this case, the z -dependence of the eigen-functions of disk oscillations are described by Hermite polynomials, $\mathcal{H}_n(z/H)$, n specifying the node number in the vertical direction. The horizontal displacements associated with the oscillations, $\boldsymbol{\xi}_\perp^{(0)}$, are then described by

$$\xi_{\perp}^{(0)} = \mathcal{H}_n \exp[i(\omega t - m\varphi)] \hat{\xi}_{\perp}^{(0)}(r) \quad (28)$$

and that in the vertical direction, $\xi_z^{(0)}$, is

$$\xi_z^{(0)} = \mathcal{H}_{n-1} \exp[i(\omega t - m\varphi)] \hat{\xi}_z^{(0)}(r). \quad (29)$$

Here, ξ_{\perp} is an abbreviation of the horizontal displacement vector (ξ_r, ξ_{φ}) and m is the number of arms in the azimuthal direction. The oscillations are now classified by a set of m and n . Furthermore, for a set of (m, n) , we have two kinds of oscillations, which are p-mode oscillations and g-mode ones. The formers are oscillations of $(\omega - m\Omega)^2 > n\Omega$ and the latters are those of $(\omega - m\Omega)^2 < \kappa^2$ (see e.g., Kato et al. 1998; Kato 2001). The p-mode oscillations start from $n = 0$, while the g-mode ones start from $n = 1$. In the framework of the present approximations, the p-mode oscillations of $n = 0$ are purely horizontal. In order to make it clear, the coefficient n has been attached to equation (29).

In addition to the oscillations mentioned above, the unperturbed disk is assumed to be deformed by a global standing ($\omega = 0$) pattern of a warp, ξ^w , which can be approximated in the lowest approximation to be (e.g., Kato 2003)

$$\xi_r^w = \xi_{\varphi}^w = 0 \quad (30)$$

and

$$\xi_z^w = \mathcal{H}_0 \exp(-i\varphi) \eta(r). \quad (31)$$

The present warp corresponds to a radially long wavelength perturbation with $n = 1$ and $m = 1$. Here and hereafter, the superscript w is used to represent the quantities associated with the warp.

3.2. Dispersion Relation

As a preparation to solve the inhomogeneous wave equation (17), we discuss here the homogeneous part of the equation. The homogeneous part is generally a set of partial differential equations. In some cases, however, the homogeneous equation becomes a set of algebraic equations, and thus the inhomogeneous non-linear equation (17) becomes manageable. As such a case, we discuss the case where the wavelength of perturbations is sufficiently short compared with the radius of the disk. This approximation is allowed, except for some special situations, since we consider geometrically thin disks.

Here, we assume that $\xi \propto \exp(ikr)$ and $kr \gg 1$. Since the z-dependences of ξ are given by equations (28) and (29), using equations (15) and (25) and the characteristics of the Hermite polynomials we have, after some manipulations, that the homogeneous part of equation (17) is expressed as

$$[-(\omega - m\Omega)^2 + \kappa^2 - 4\Omega^2] \hat{\xi}_r^{(0)} - i2\Omega(\omega - m\Omega) \hat{\xi}_{\varphi}^{(0)} + (kH)\Omega_{\perp}^2 \left[(kH) \hat{\xi}_r^{(0)} + i \hat{\xi}_z^{(0)} \right] = 0, \quad (32)$$

$$-(\omega - m\Omega)^2 \hat{\xi}_{\varphi}^{(0)} + i2\Omega(\omega - m\Omega) \hat{\xi}_r^{(0)} = 0, \quad (33)$$

and

$$[-(\omega - m\Omega)^2 + n\Omega_\perp^2]\hat{\xi}_z^{(0)} - in(kH)\Omega_\perp^2\hat{\xi}_r^{(0)} = 0. \quad (34)$$

In these equations the terms with c_s^2 come from the Eulerian pressure variations (see the next paragraph). If these terms are neglected, the above equations are those derived by the particle approximations, and thus the horizontal motions and the vertical motions are uncoupled. This is also shown clearly by deriving the dispersion relation (i.e., the solvability condition) from the set of equations (32)–(34), which is

$$[(\omega - m\Omega)^2 - \kappa^2][(\omega - m\Omega)^2 - n\Omega_\perp^2] = c_s^2 k^2 (\omega - m\Omega)^2. \quad (35)$$

It will be instructive to note here that for a polytropic gas we can derive after manipulations that $\mathbf{P}_1(\boldsymbol{\xi})$ is related to $\rho_0 \nabla h_1$ by

$$\mathbf{P}_{(1)}(\boldsymbol{\xi}) = \rho_0 \nabla h_1 + \rho_0 (\boldsymbol{\xi} \cdot \nabla) \left(\frac{1}{\rho_0} \nabla p_0 \right), \quad (36)$$

where $h_1 \equiv p_1/\rho_0$ is the Eulerian pressure variation, p_1 , being normalized by ρ_0 . In the framework of the present approximations, $\partial h_1/\partial r = c_s^2[k^2\hat{\xi}_r^{(0)} + i(k/H)\hat{\xi}_z^{(0)}]\mathcal{H}_n$ and $\partial h_1/\partial z = [n\Omega_\perp^2\hat{\xi}_z^{(0)} - inc_s^2(k/H)\hat{\xi}_r^{(0)}]\mathcal{H}_{n-1}$.

4. The First Stage of Coupling between Warp and Oscillations

We here examine how the disk oscillations and the warp described in section 3 are coupled. The procedures of examinations are the same as those in Paper I and outlined in subsection 2.2. That is, we assume that the amplitude of oscillations is so small that their non-linear effects on the oscillations, themselves, are negligible. The amplitude of the warp, on the other hand, is so large that the effects of the warp on the oscillations are non-negligible. We examine them successively, as is shown in figure 1. The first step of their interactions is direct non-linear coupling between the warp and the oscillations, which brings about intermediate oscillations of $(m \pm 1, n \pm 1)$ with frequency ω (see figure 1). To these intermediate oscillations the disk responds resonantly at a radius where the dispersion relation to the intermediate oscillations is satisfied. After having this resonant interaction, the intermediate oscillations interact with the warp to feedback to the original oscillations of (m, n) with ω (see figure 1). This non-linear feedback to the original oscillations through a resonant coupling amplifies or dampens the original oscillations.

In this section we consider the first stage of the above couplings. The intermediate waves resulting from this coupling are expressed by attaching a superscript (1) as $\boldsymbol{\xi}^{(1)}$. As mentioned before, the coupling has two paths. One is the path where the azimuthal wavenumber of the intermediate oscillations is $m + 1$, and the other is the path with $m - 1$. To distinguish $\boldsymbol{\xi}^{(1)}$ in these two paths, we attach the subscript + to $\boldsymbol{\xi}^{(1)}$ as $\boldsymbol{\xi}_+^{(1)}$ in the former case and the subscript – in the latter case as $\boldsymbol{\xi}_-^{(1)}$. From equation (17) the inhomogeneous wave equation describing $\boldsymbol{\xi}_\pm^{(1)}$ is found to be

$$-\omega^2 \rho_0 \boldsymbol{\xi}_{\pm}^{(1)} + 2i\omega \rho_0 (\mathbf{u}_0 \cdot \nabla) \boldsymbol{\xi}_{\pm}^{(1)} + \mathbf{L}(\boldsymbol{\xi}_{\pm}^{(1)}) = \rho_0 \mathbf{C}_{\pm}^{(1)}, \quad (37)$$

where

$$\mathbf{C}_+^{(1)} = \mathbf{C}(\boldsymbol{\xi}^{(0)}, \boldsymbol{\xi}^w) \quad \text{and} \quad \mathbf{C}_-^{(1)} = \mathbf{C}(\boldsymbol{\xi}^{(0)}, \boldsymbol{\xi}^{w*}). \quad (38)$$

Equation (37) represents two equations. One is the equation for the upper sign (it is + in the present case) and the other is that for the lower sign (e.g., -). Both equations are written in one set, since they have similar forms and can be treated in parallel.

Our purpose here is to solve this inhomogeneous wave equation (37) to obtain $\boldsymbol{\xi}_+^{(1)}$ and $\boldsymbol{\xi}_-^{(1)}$. Although this equation can be formally solved by using a Green function, it is too complicated and not practical. Hence, we are satisfied here to solve the equation by introducing the approximations of vertically isothermal disks (see section 3). In this case, concerning the functional forms in the vertical direction, the feedbacks to the original oscillations occur through two paths. One is a path through $n \rightarrow n-1 \rightarrow n$ (lower path). The other is through the path of $n \rightarrow n+1 \rightarrow n$ (upper path). In the former case, the intermediate oscillations in the horizontal direction, $\boldsymbol{\xi}_{\perp}^{(1)}$, are proportional to $\mathcal{H}_{n-1}(z/H)$, while it is proportional to $\mathcal{H}_{n+1}(z/H)$ in the latter case. [It is noted that the vertical displacement, $\xi_z^{(1)}$, associated with the intermediate oscillations are proportional to $\mathcal{H}_{n-2}(z/H)$ and $\mathcal{H}_n(z/H)$.] In order to treat these two cases separately, we attach the subscript \tilde{n} to $\boldsymbol{\xi}_{\pm}^{(1)}$ as $\boldsymbol{\xi}_{\pm, \tilde{n}}^{(1)}$, where \tilde{n} represents $n-1$ or $n+1$. Then, the r -, φ -, and z -components of $\boldsymbol{\xi}_{\pm, \tilde{n}}^{(1)}$ are written as

$$\xi_{r, \pm, \tilde{n}}^{(1)} = \mathcal{H}_{\tilde{n}} \exp\{i[\omega t - (m \pm 1)\varphi]\} \hat{\xi}_{r, \pm, \tilde{n}}^{(1)}(r), \quad (39)$$

$$\xi_{\varphi, \pm, \tilde{n}}^{(1)} = \mathcal{H}_{\tilde{n}} \exp\{i[\omega t - (m \pm 1)\varphi]\} \hat{\xi}_{\varphi, \pm, \tilde{n}}^{(1)}(r), \quad (40)$$

$$\xi_{z, \pm, \tilde{n}}^{(1)} = \mathcal{H}_{\tilde{n}-1} \exp\{i[\omega t - (m \pm 1)\varphi]\} \hat{\xi}_{z, \pm, \tilde{n}}^{(1)}(r). \quad (41)$$

It should be noted here that in equation (41) subscript \tilde{n} is attached to $\xi_{z, \pm}^{(1)}$, although it is proportional to $\mathcal{H}_{\tilde{n}-1}$. We adopt this notation in order to clarify that $\xi_{r, \pm, \tilde{n}}^{(1)}$, $\xi_{\varphi, \pm, \tilde{n}}^{(1)}$, and $\xi_{z, \pm, \tilde{n}}^{(1)}$ are one of the sets of solutions for the same intermediate oscillations.

Using equations (39)–(41) and the procedures used to derive the wave equations for oscillations $\boldsymbol{\xi}^{(0)}$ [equations (32)–(34)], we can write the equations corresponding to equation (21) as

$$\begin{aligned} & \{ -[\omega - (m \pm 1)\Omega]^2 + (\kappa^2 - 4\Omega^2) \} \hat{\xi}_{r, \pm, \tilde{n}}^{(1)} - i2\Omega[\omega - (m \pm 1)\Omega] \hat{\xi}_{\varphi, \pm, \tilde{n}}^{(1)} \\ & + k^2 c_s^2 \hat{\xi}_{r, \pm, \tilde{n}}^{(1)} + ik \frac{c_s^2}{H} \hat{\xi}_{z, \pm, \tilde{n}}^{(1)} = \hat{C}_{r, \pm, \tilde{n}}^{(1)}, \end{aligned} \quad (42)$$

$$-[\omega - (m \pm 1)\Omega]^2 \hat{\xi}_{\varphi, \pm, \tilde{n}}^{(1)} + i2\Omega[\omega - (m \pm 1)\Omega] \hat{\xi}_{r, \pm, \tilde{n}}^{(1)} = \hat{C}_{\varphi, \pm, \tilde{n}}^{(1)}, \quad (43)$$

$$\{ -[\omega - (m \pm 1)\Omega]^2 + \tilde{n}\Omega_{\perp}^2 \} \hat{\xi}_{z, \pm, \tilde{n}}^{(1)} - ikn \frac{c_s^2}{H} \hat{\xi}_{r, \pm, \tilde{n}}^{(1)} = \hat{C}_{z, \pm, \tilde{n}}^{(1)}, \quad (44)$$

where $\hat{C}_{r, \pm, \tilde{n}}^{(1)}$ and $\hat{C}_{\varphi, \pm, \tilde{n}}^{(1)}$ are the parts of $C_{r, \pm, \tilde{n}}^{(1)}$ and $C_{\varphi, \pm, \tilde{n}}^{(1)}$ that are proportional to $\exp\{i(\omega t - (m \pm 1)\varphi)\} \mathcal{H}_{\tilde{n}}(z/H)$, respectively, i.e.,

$$C_{r,\pm,\tilde{n}}^{(1)} = \mathcal{H}_{\tilde{n}}(z/H) \exp\{i(\omega t - (m \pm 1)\varphi)\} \hat{C}_{r,\pm,\tilde{n}}^{(1)}, \quad (45)$$

$$C_{\varphi,\pm,\tilde{n}}^{(1)} = \mathcal{H}_{\tilde{n}}(z/H) \exp\{i(\omega t - (m \pm 1)\varphi)\} \hat{C}_{\varphi,\pm,\tilde{n}}^{(1)}. \quad (46)$$

Similarly,

$$C_{z,\pm,\tilde{n}}^{(1)} = \mathcal{H}_{\tilde{n}-1}(z/H) \exp\{i(\omega t - (m \pm 1)\varphi)\} \hat{C}_{z,\pm,\tilde{n}}^{(1)}. \quad (47)$$

Detailed expressions for $\hat{C}_{r,\pm,\tilde{n}}^{(1)}$, $\hat{C}_{\varphi,\pm,\tilde{n}}^{(1)}$, and $\hat{C}_{z,\pm,\tilde{n}}^{(1)}$ are given in appendix 2.

Equation (42)–(44) are easily solved with respect to $\hat{\xi}^{(1)}$ to obtain

$$\hat{\xi}_{r,\pm,\tilde{n}}^{(1)} = \frac{1}{D_{\pm,\tilde{n}}} \hat{\zeta}_{r,\pm,\tilde{n}}^{(1)}, \quad \hat{\xi}_{\varphi,\pm,\tilde{n}}^{(1)} = \frac{1}{D_{\pm,\tilde{n}}} \hat{\zeta}_{\varphi,\pm,\tilde{n}}^{(1)}, \quad \text{and} \quad \hat{\xi}_{z,\pm,\tilde{n}}^{(1)} = \frac{1}{D_{\pm,\tilde{n}}} \hat{\zeta}_{z,\pm,\tilde{n}}^{(1)}, \quad (48)$$

where

$$\begin{aligned} \hat{\zeta}_{r,\pm,\tilde{n}}^{(1)} = & -[(\omega - (m \pm 1)\Omega)^2 - \tilde{n}\Omega_{\perp}^2] \left[\hat{C}_{r,\pm,\tilde{n}}^{(1)} - i \frac{2\Omega}{\omega - (m \pm 1)\Omega} \hat{C}_{\varphi,\pm,\tilde{n}}^{(1)} \right] \\ & - i(kH)\Omega_{\perp}^2 \hat{C}_{z,\pm,\tilde{n}}^{(1)}, \end{aligned} \quad (49)$$

$$\hat{\zeta}_{\varphi,\pm,\tilde{n}}^{(1)} = i \frac{2\Omega}{\omega - (m \pm 1)\Omega} \hat{\zeta}_{r,\pm,\tilde{n}}^{(1)}, \quad (50)$$

$$\hat{\zeta}_{z,\pm,\tilde{n}}^{(1)} = i\tilde{n}\Omega_{\perp}^2 \left\{ kH \left[\hat{C}_{r,\pm,\tilde{n}}^{(1)} - i \frac{2\Omega}{\omega - (m \pm 1)\Omega} \hat{C}_{\varphi,\pm,\tilde{n}}^{(1)} \right] + i \frac{[\omega - (m \pm 1)\Omega]^2 - \kappa^2}{[\omega - (m \pm 1)\Omega]^2} \hat{C}_{z,\pm,\tilde{n}}^{(1)} \right\}. \quad (51)$$

Furthermore, $D_{\pm,\tilde{n}}$ is defined as

$$D_{\pm,\tilde{n}} = \left\{ [\omega - (m \pm 1)\Omega]^2 - \kappa^2 \right\} \left\{ [\omega - (m \pm 1)\Omega]^2 - \tilde{n}\Omega_{\perp}^2 \right\} - k^2 c_s^2 [\omega - (m \pm 1)\Omega]^2. \quad (52)$$

An important characteristics of the intermediate mode, $\xi^{(1)}$, is that it becomes infinite at the radius where $D_{\pm,\tilde{n}} = 0$. This implies that the disk responds resonantly to the intermediate oscillations at these radii. Since the pressure terms in equation (52) are usually small, $D_{\pm,\tilde{n}} = 0$ is realized at radii close to $[\omega - (m \pm 1)\Omega]^2 - \kappa^2 \sim 0$ or $[\omega - (m \pm 1)\Omega]^2 - \tilde{n}\Omega_{\perp}^2 \sim 0$. The former resonances are hereafter called horizontal resonances, while the latter ones are vertical resonances.

5. Resonant Radii and Resonant Frequencies

The resonant radii where the disk responds resonantly to the intermediate oscillations must be within the propagation region of the original oscillations. This condition has been extensively examined by Paper I. We mention here a part of the results.

There are two kinds of oscillations on disks, i.e., the p-mode and g-mode oscillations. Furthermore, resonances have two types, i.e., horizontal and vertical resonances. Combinations of them give us three types of resonances: i) horizontal resonances of the g-mode oscillations, ii) vertical resonances of the g-mode oscillations, and iii) horizontal resonances of the p-mode oscillations. It should be noted that vertical resonances of the p-mode oscillations are absent.

As a demonstration, we present here where horizontal resonances of the g-mode oscillations occur and how much their frequencies are when $n = 1$ and the path of the coupling is $n \rightarrow n + 1$ and n (i.e., $\tilde{n} = 2$). As equation (52) shows, the horizontal resonances occur near to

$$\omega - (m \pm 1)\Omega \sim \kappa \quad \text{or} \quad \omega - (m \pm 1)\Omega \sim -\kappa. \quad (53)$$

The propagation of the g-mode oscillations with frequency ω , on the other hand, is bound in the region of $-\kappa < \omega - m\Omega < \kappa$ [see dispersion relation (35)]. Since we are interested in oscillations whose frequencies are near to the boundaries of the propagation region, we require that

$$\omega - m\Omega \sim -\kappa \quad \text{or} \quad \omega - m\Omega \sim \kappa. \quad (54)$$

Requirements (53) and (54) are simultaneously satisfied when $\Omega \sim 2\kappa$. That is, in the case of the plus sign of $m \pm 1$, they are satisfied when $\omega - (m + 1)\Omega \sim -\kappa$ and $\omega - m\Omega \sim \kappa$, and in the case of the minus sign of $m \pm 1$, $\omega - (m - 1)\Omega \sim \kappa$ and $\omega - m\Omega \sim -\kappa$. The requirement $\Omega = 2\kappa$ is realized at $r \sim 4.0r_g$ when the Schwarzschild metric is adopted, where r_g is the Schwarzschild radius, defined by $r_g = 2GM/c^2$, M being the mass of the central object. The frequencies of the oscillations at the radius are $m\Omega \mp \kappa$. In the case of $m = 2$ they are 0.1875 and 0.313 in units of $(GM/r_g^3)^{1/2}$ (see Paper I).

The above discussions are only for the case of the horizontal resonances of the g-mode oscillations with $n = 1$ and $\tilde{n} = 2$. Discussions for other types of resonances (Paper I) show that resonances can occur at, and only at, the radii where

$$\kappa = 0, \quad \sqrt{2}\Omega_\perp - \Omega = \kappa, \quad \Omega = 2\kappa, \quad \sqrt{3}\Omega_\perp - \Omega = \kappa, \quad (55)$$

depending on the types of the resonances and modes of oscillations. The radii satisfying the above requirements in equation (55) are, in turn,

$$r = 3r_g, \quad r = 3.62r_g, \quad r = 4.0r_g, \quad \text{and} \quad r = 6.46r_g. \quad (56)$$

Since more detailed discussions concerning the resonant radii and the resonant frequencies at these radii are given by Paper I, we proceed here to the issue which resonances lead to amplifications of the oscillations.

To proceed further, however, there is an important issue to be noted here, which is the sign of the ratio of $\omega - (m \pm 1)\Omega$ and $\omega - m\Omega$ at the resonance point. This is important to discuss whether the resonances lead to amplification or to damping, as will become clear in section 7. The sign is negative in the case demonstrated above. Careful examinations show that the ratio is always negative in horizontal resonances of all g-mode oscillations, while it is positive in vertical resonances of all g-mode oscillations and horizontal resonances of p-mode oscillations (except for $n = 0$).

6. The Second Stage of Coupling

The next issue is to study whether the resonances discussed in the previous sections act so as to amplify the original oscillations or not. For this purpose, the non-linear coupling between the intermediate oscillations $\xi^{(1)}$ and the warp ξ^w is discussed. The coupling brings about oscillations of the same form as the original oscillations, i.e., the r - and φ - components of the displacements of the resulting oscillations are proportional to $\exp[i(\omega t - m\varphi)]\mathcal{H}_n(z/H)$ and the z -component is proportional to $\exp[i(\omega t - m\varphi)]\mathcal{H}_{n-1}(z/H)$. This feedback acts so as to amplify or dampen the original oscillations, depending on the phase relations at the resonance points.

Now, we start from equation (24). The equation has a clear physical meaning. The left-hand side of the equation can be reduced to

$$-2i\omega_i \int (\omega - m\Omega) \rho_0 (\xi_r^{(0)*} \xi_r^{(0)} + \xi_z^{(0)*} \xi_z^{(0)}) dV, \quad (57)$$

when an approximate relation between $\xi_r^{(0)}$ and $\xi_\varphi^{(0)}$, i.e.,

$$i(\omega - m\Omega)\xi_\varphi^{(0)} + 2\Omega\xi_r^{(0)} = 0, \quad (58)$$

which is the φ -component of the equation of motion, is used. If vertical integration is performed, equation (57) can be written as

$$-2i\omega_i (2\pi)^{1/2} H \int (\omega - m\Omega) \rho_{00} [n\hat{\xi}_r^{(0)*} \hat{\xi}_r^{(0)} + (n-1)\hat{\xi}_z^{(0)*} \hat{\xi}_z^{(0)}] 2\pi r dr. \quad (59)$$

We now remember that the wave energy is known to be defined by (e.g., Kato 2001)

$$E = \frac{1}{2}\omega \int (\omega - m\Omega) \rho_0 (\xi_r^{(0)*} \xi_r^{(0)} + \xi_z^{(0)*} \xi_z^{(0)}) dV. \quad (60)$$

[In Kato (2001) E is written by using the Eulerian velocity perturbations, u_r and u_z , instead of the Lagrangian displacements.] Hence, equation (57) is

$$-4i \frac{\omega_i}{\omega_0} E, \quad (61)$$

and is related to the rate of change of the wave energy.

The right-hand side of equation (24) represents the work done on the original oscillations through non-linear couplings with a warp. As mentioned before, there are four paths of the feedback to the original oscillations, i.e., two paths of $m \rightarrow m \pm 1 \rightarrow m$ and two paths of $n \rightarrow n \pm 1 \rightarrow n$. We treat these four paths separately. Equation (24) shows that for the coupling of $m \rightarrow m + 1 \rightarrow m$, the rate of energy change of the oscillations is given by

$$-4i \frac{\omega_i}{\omega_0} E = \Im \int \rho_0 \xi^{(0)*} C_{+, \tilde{n}}^{(2)}(\xi_{+, \tilde{n}}^{(1)}, \xi^{w*}) dV, \quad (62)$$

while

$$-4i \frac{\omega_i}{\omega_0} E = \Im \int \rho_0 \xi^{(0)*} C_{-, \tilde{n}}^{(2)}(\xi_{-, \tilde{n}}^{(1)}, \xi^w) dV, \quad (63)$$

when the path is $m \rightarrow m-1 \rightarrow m$. Here, $\mathbf{C}_{+, \tilde{n}}^{(2)}$, for example, represents the coupling between $\xi_{+, \tilde{n}}^{(1)}$ and ξ^{w*} . To make clear that this is the second stage of the coupling and that the path is $m \rightarrow m+1 \rightarrow m$, the superscript (2) and the subscript + have been attached to \mathbf{C} .

When integrations on the right-hand side of equations (62) and (63) are performed, we should first remember that among various terms of $\mathbf{C}^{(2)}$, we need only those terms proportional to $\mathcal{H}_n(z/H)$ for $\mathbf{C}_{\perp}^{(2)}$ and to $\mathcal{H}_{n-1}(z/H)$ for $\mathbf{C}_z^{(2)}$. This is because $\xi^{(0)}$ and $\xi_z^{(0)}$ are proportional to $\mathcal{H}_n(z/H)$ and $\mathcal{H}_{n-1}(z/H)$, respectively, and Hermite polynomials of different orders are orthogonal to each other. Second, we should consider that $\xi^{(1)}$'s have poles at the radii where $D=0$ is realized, and the imaginary parts of the integrations (62) and (63) come from integration around the poles. Related to this, when we calculate $\mathbf{C}^{(2)}(\xi^{(1)}, \xi^{w*})$, the term $1/D$ in $\xi^{(1)}$ can be moved outside of $\mathbf{C}^{(2)}$ as $(1/D)\mathbf{C}^{(2)}(\xi^{(1)}, \xi^{w*})$.

Based on these considerations, we write the $\mathbf{C}^{(2)}$'s as

$$\mathbf{C}_{\perp, +, \tilde{n}}^{(2)} = \frac{1}{D_{+, \tilde{n}}} \mathcal{H}_n(z/H) \exp\{i(\omega t - m\varphi)\} \hat{\mathbf{C}}_{\perp, +, \tilde{n}}^{(2)}(\hat{\zeta}_{+, \tilde{n}}, \hat{\eta}^*), \quad (64)$$

$$\mathbf{C}_{z, +, \tilde{n}}^{(2)} = \frac{1}{D_{+, \tilde{n}}} \mathcal{H}_{n-1}(z/H) \exp\{i(\omega t - m\varphi)\} \hat{\mathbf{C}}_{z, +, \tilde{n}}^{(2)}(\hat{\zeta}_{+, \tilde{n}}, \hat{\eta}^*). \quad (65)$$

Then, the right-hand side of equation (62), for example, can be written as

$$\left\{ (2\pi)^{3/2} r H \rho_{00} \left[n! \hat{\xi}_{\perp}^{(0)*} \cdot \hat{\mathbf{C}}_{\perp, +, \tilde{n}}^{(2)}(\hat{\zeta}_{+, \tilde{n}}, \hat{\eta}^*) + (n-1)! \hat{\xi}_z^{(0)*} \cdot \hat{\mathbf{C}}_{z, +, \tilde{n}}^{(2)}(\hat{\zeta}_{+, \tilde{n}}, \hat{\eta}^*) \right] \right\}_c \Im \left(\int \frac{dr}{D_{+, \tilde{n}}} \right), \quad (66)$$

where the subscript c denotes the value at the resonance radius, and the expressions for $\hat{\mathbf{C}}_{\perp, +, \tilde{n}}^{(2)}$ and $\hat{\mathbf{C}}_{z, +, \tilde{n}}^{(2)}$ are given in appendix 3. The right-hand side of equation (63) has the same form as equation (66), except that $\hat{\mathbf{C}}_{\perp, +, \tilde{n}}^{(2)}(\hat{\zeta}_{+, \tilde{n}}, \hat{\eta}^*)$ and $\hat{\mathbf{C}}_{z, +, \tilde{n}}^{(2)}(\hat{\zeta}_{+, \tilde{n}}, \hat{\eta}^*)$ are replaced by $\hat{\mathbf{C}}_{\perp, -, \tilde{n}}^{(2)}(\hat{\zeta}_{-, \tilde{n}}, \hat{\eta})$ and $\hat{\mathbf{C}}_{z, -, \tilde{n}}^{(2)}(\hat{\zeta}_{-, \tilde{n}}, \hat{\eta})$. Furthermore, D_+ in equation (66) is replaced by D_- . Expressions for $\hat{\mathbf{C}}_{\perp, -, \tilde{n}}^{(2)}$ and $\hat{\mathbf{C}}_{z, -, \tilde{n}}^{(2)}$ are also given in appendix 3.

To perform integration around the poles, we must be careful about the integration path, so that causality is satisfied (e.g., Kato 2003). Let us consider the horizontal and vertical resonances separately. For the horizontal resonances we have $[\omega - (m \pm 1)\Omega]^2 - \kappa^2 \sim 0$ and around the resonance radius, r_c , the first term of the Taylor expansion of $D_{\pm, \tilde{n}}$ gives

$$D_{\pm, \tilde{n}} = 2(\tilde{n}\Omega_{\perp}^2 - \kappa^2) G_{H, \pm} \left[\frac{r - r_c}{r} - i \frac{\omega - (m \pm 1)\Omega}{G_{H, \pm}} \omega_i \right], \quad (67)$$

where

$$G_{H, \pm} = \left\{ (m \pm 1)\Omega [\omega - (m \pm 1)\Omega] \frac{d \ln \Omega}{d \ln r} + \kappa^2 \frac{d \ln \kappa}{d \ln r} \right\}_c. \quad (68)$$

Considering these expressions and the requirement of causality, we have

$$\int \frac{1}{D_{\pm, \tilde{n}}} dr = -i\pi \frac{r_c}{2(\tilde{n}\Omega_{\perp}^2 - \kappa^2)_c |G_{H, \pm}|} \text{sign}[\omega - (m \pm 1)\Omega]_c. \quad (69)$$

Here and hereafter, subscript c denotes the values at the resonance radius.

In the case of vertical resonances, $[\omega - (m \pm 1)\Omega]^2 - \tilde{n}\Omega_\perp^2 \sim 0$ and around the resonance radius, r_c , we have

$$D_{\pm, \tilde{n}} = -2(\tilde{n}\Omega_\perp^2 - \kappa^2)G_{V, \pm, \tilde{n}} \left[\frac{r - r_c}{r} - i \frac{\omega - (m \pm 1)\Omega}{G_{V, \pm, \tilde{n}}} \omega_i \right], \quad (70)$$

where

$$G_{V, \pm, \tilde{n}} = \left\{ (m \pm 1)\Omega [\omega - (m \pm 1)\Omega] \frac{d \ln \Omega}{d \ln r} + 2\tilde{n} \left(\Omega_\perp \frac{d \Omega_\perp}{d \ln r} \right) \right\}_c. \quad (71)$$

Similarly, we have

$$\int \frac{1}{D_{\pm, \tilde{n}}} dr = i\pi \frac{r_c}{2(\tilde{n}\Omega_\perp^2 - \kappa^2)_c |G_{V, \pm}|} \text{sign}[\omega - (m \pm 1)\Omega]_c. \quad (72)$$

Taking these considerations into account, we can write equation (62) as

$$-2\omega_i = -\frac{\pi}{4(-\kappa^2 + \tilde{n}\Omega^2)_c} |G_{H, +, \tilde{n}}|_c \frac{\text{sign}[\omega - (m + 1)\Omega]_c}{(\omega - m\Omega)_c} \frac{\tilde{W}_c}{\tilde{E}}, \quad (73)$$

where \tilde{W} is related to the work done on oscillations, and is

$$\tilde{W} = n! \hat{\xi}_{r, +, \tilde{n}}^{(0)} \hat{C}_{r, +, \tilde{n}}^{(2)} + n! \hat{\xi}_{\varphi, +, \tilde{n}}^{(0)} \hat{C}_{\varphi, +, \tilde{n}}^{(2)} + (n - 1)! \hat{\xi}_{z, +, \tilde{n}}^{(0)} \hat{C}_{z, +, \tilde{n}}^{(2)} \quad (74)$$

and

$$\tilde{E} = \int \frac{r H \rho_{00}}{r_c H_c \rho_{00} r_c} \frac{\omega - m\Omega}{\omega - m\Omega_c} \left(n! |\hat{\xi}_r^{(0)}|^2 + (n - 1)! |\hat{\xi}_z^{(0)}|^2 \right) \frac{dr}{r_c}. \quad (75)$$

In the case of $m \rightarrow m - 1 \rightarrow m$, an expression for the growth rate is similar to equation (73). The differences are that the arguments of $\hat{C}_{-, \tilde{n}}^{(2)}$ are now $\hat{\xi}_{-, \tilde{n}}^{(1)}$ and $\hat{\eta}$.

Next, we should mention the case of vertical resonances. Derivations of expressions for the growth rate are quite parallel with the case of horizontal resonances, and we have

$$-2\omega_i = \frac{\pi}{4(-\kappa^2 + \tilde{n}\Omega^2)_c} |G_{V, +, \tilde{n}}|_c \frac{\text{sign}[\omega - (m + 1)\Omega]_c}{(\omega - m\Omega)_c} \frac{\tilde{W}_c}{\tilde{E}}. \quad (76)$$

We should especially notice that the sign is different from equation (73).

7. Growth Rate of Resonant Oscillations

In this section, the growth (or damping) rates of resonant oscillations are calculated using equations (73) and (76). As discussed in section 5, there are three kinds of resonances: i) horizontal and ii) vertical resonances of g-mode oscillations and iii) horizontal resonances of p-mode oscillations. These resonances are discussed here separately. It is noted that the oscillation modes of $n = 0$ are p-modes alone. These p-modes are similar in dynamical behaviors with g-mode oscillations of $n \geq 1$. Hence, the p-modes of $n = 0$ are treated hereafter together with g-mode oscillations of $n \geq 1$. In other words, when we mention p-mode oscillations, they are p-mode oscillations of $n \geq 1$. Two basic approximations are introduced here. The first one is that $c_s^2 k^2$ is much smaller than the square of the rotational frequency, Ω^2 , which means that we adopt $(kH)^2 \ll 1$. This is a natural approximation in treating disk oscillations in geometrically

thin disks. Introduction of this approximation implies that we are interested in resonances that occur near to both boundaries of the propagation and resonance regions. That is, we consider resonances where $[(\omega - m\Omega)^2 - \kappa^2][(\omega - m\Omega)^2 - n\Omega_\perp^2] \sim 0$ and $\{[\omega - (m \pm 1)\Omega]^2 - \kappa^2\}\{[\omega - (m \pm 1)\Omega]^2 - \tilde{n}\Omega_\perp^2\} \sim 0$ are simultaneously realized. The second approximation we adopt here is a local approximation of $(kr)^2 \gg 1$. This approximation is relevant, except for just the boundaries of the resonance and propagation regions, since we are treating geometrically thin disks.

7.1. G-Mode Oscillations

First, we summarize the relations among $\hat{\xi}_r^{(0)}$, $\hat{\xi}_\varphi^{(0)}$, and $\hat{\xi}_z^{(0)}$ in g-mode oscillations. In g-mode oscillations, $(\omega - m\Omega)^2 - \kappa^2$ is close to zero, but can be approximated as $(kH)^2\Omega_\perp^2[\kappa^2/(\kappa^2 - n\Omega_\perp^2)]$ by using the dispersion relation (35). Hence, from equation (34) we have a relation between $\hat{\xi}_r^{(0)}$ and $\hat{\xi}_z^{(0)}$ as

$$\hat{\xi}_z^{(0)} = -i(kH)\frac{n\Omega_\perp^2}{\kappa^2 - n\Omega_\perp^2}\hat{\xi}_r^{(0)}. \quad (77)$$

A relation between $\hat{\xi}_\varphi^{(0)}$ and $\hat{\xi}_r^{(0)}$ is, from equation (33),

$$\hat{\xi}_\varphi^{(0)} = i\frac{2\Omega}{\omega - m\Omega}\hat{\xi}_r^{(0)}. \quad (78)$$

These relations show that in g-mode oscillations, $\hat{\xi}_z^{(0)}$ is smaller than $\hat{\xi}_r^{(0)}$ and $\hat{\xi}_\varphi^{(0)}$ by a factor of (kH) .

Since in the paths of $n \rightarrow n+1 \rightarrow n$ (i.e., $\tilde{n} = n+1$) and $n \rightarrow n-1 \rightarrow n$ (i.e., $\tilde{n} = n-1$), expressions for $\hat{C}^{(1)}$'s are different, we treat these two cases separately. In the case of the upper path ($\tilde{n} = n+1$), neglecting small-order quantities, we have from appendix 2

$$\hat{C}_{r,+,n+1}^{(1)} = i(kH)\Omega_\perp^2\hat{\xi}_r^{(0)}\left(\frac{d\eta}{dr} + \frac{2\Omega}{\omega - m\Omega}\frac{\eta}{r}\right), \quad (79)$$

$$\hat{C}_{z,+,n+1}^{(1)} = \Omega_\perp^2\hat{\xi}_r^{(0)}\left[-\frac{d\ln\Omega_\perp^2}{dr}\eta + n\left(\frac{d\eta}{dr} + \frac{2\Omega}{\omega - m\Omega}\frac{\eta}{r}\right)\right]. \quad (80)$$

Here, we do not present $\hat{C}_{\varphi,+,n+1}^{(1)}$, since it is smaller than $\hat{C}_{r,+,n+1}^{(1)}$ and unnecessary hereafter. Although $\hat{C}_{r,+,n+1}^{(1)}$ is smaller than $\hat{C}_{z,+,n+1}^{(1)}$ by a factor of kH , it contributes to the final results.

In the case of the lower path, on the other hand, using expressions in appendix 2 and approximations of $kH \ll 1$ and $kr \gg 1$, we have

$$\hat{C}_{r,+,n-1}^{(1)} = \Omega_\perp^2\left\{-in(kH)\hat{\xi}_r^{(0)}\frac{d\eta}{dr} + \hat{\xi}_z^{(0)}\left(-\frac{d\ln\Omega_\perp^2}{dr}\eta + (n-1)\frac{d\eta}{dr}\right)\right\}, \quad (81)$$

$$\hat{C}_{\varphi,+,n-1}^{(1)} = -\Omega_\perp^2\frac{1}{r}\left[n(kH)\hat{\xi}_r^{(0)} + i(n-1)\hat{\xi}_z^{(0)}\right]\eta. \quad (82)$$

The term $\hat{C}_{z,+,n-1}^{(1)}$ is not presented here since it is smaller than $\hat{C}_{r,+,n-1}^{(1)}$ and $\hat{C}_{\varphi,+,n-1}^{(1)}$ by a factor of H/r , and is unnecessary hereafter.

7.1.1. Horizontal resonances of g -mode oscillations

To proceed further, we separately consider two coupling paths of $n \rightarrow n+1 \rightarrow n$ and $n \rightarrow n-1 \rightarrow n$.

(a) Coupling through the upper path ($\tilde{n} = n+1$)

In this case, we can express $\hat{\zeta}_{+,n+1}^{(1)}$ in terms of $\hat{\xi}_{+,n+1}^{(1)}$ by using equations (49)–(51) under the help of equations (79) and (80). The results are

$$\hat{\zeta}_{r,+,n+1}^{(1)} = i(kH)\Omega_{\perp}^4 \hat{\xi}_r^{(0)} \left\{ \frac{d\ln\Omega_{\perp}^2}{dr} \eta + \frac{-\kappa^2 + \Omega_{\perp}^2}{\Omega_{\perp}^2} \left(\frac{d\eta}{dr} + \frac{2\Omega}{\omega - m\Omega} \frac{\eta}{r} \right) \right\}, \quad (83)$$

$$\hat{\zeta}_{\varphi,+,n+1}^{(1)} = i \frac{2\Omega}{\omega - (m+1)\Omega} \hat{\zeta}_{r,+,n+1}^{(1)}, \quad (84)$$

$$\hat{\zeta}_{z,+,n+1}^{(1)} = i\tilde{n}(kH) \frac{\Omega_{\perp}^2}{-\kappa^2 + \tilde{n}\Omega_{\perp}^2} \hat{\zeta}_{r,+,n+1}^{(1)}. \quad (85)$$

This shows that $\hat{\zeta}_{z,+,n+1}^{(1)}$ is smaller than $\hat{\zeta}_{\perp,+,n+1}^{(1)}$ by a factor of kH , but it is necessary in deriving \tilde{W} .

The next step is to calculate $\hat{C}_{+,n+1}^{(2)}$ by using equations (83)–(85). By consulting the expressions for $\hat{C}(\hat{\xi}, \hat{\xi})$ given in appendix 2, we can derive $\hat{C}(\hat{\xi}^{(1)}, \hat{\eta}^*)$. Considering the order of each term, we have

$$\hat{C}_{r,+,n+1}^{(2)} = -i\tilde{n}(kH)\Omega_{\perp}^2 \hat{\zeta}_{r,+,n+1}^{(1)} \frac{d\eta^*}{dr} + \Omega_{\perp}^2 \hat{\zeta}_{z,+,n+1}^{(1)} \left(-\frac{d\ln\Omega_{\perp}^2}{dr} \eta^* + n \frac{d\eta^*}{dr} \right), \quad (86)$$

$$\hat{C}_{\varphi,+,n+1}^{(2)} = \frac{\Omega_{\perp}^2}{r} \left[\tilde{n}(kH) \hat{\zeta}_{r,+,n+1}^{(1)} + in \hat{\zeta}_{z,+,n+1}^{(1)} \right] \eta^*. \quad (87)$$

Here, $\hat{C}_{z,+,n+1}^{(2)}$ is omitted, since it does not contribute to \tilde{W} . Using the above expressions, we finally have, after lengthy manipulations, a simple expression:

$$\tilde{W} = n! \left(\hat{\xi}_r^{(0)} \hat{C}_{r,+,n+1}^{(2)} + \hat{\xi}_{\varphi}^{(0)} \hat{C}_{\varphi,+,n+1}^{(2)} \right) = \frac{\tilde{n}!}{-\kappa^2 + \tilde{n}\Omega_{\perp}^2} |\hat{\zeta}_{r,+,n+1}^{(1)}|^2. \quad (88)$$

(b) Coupling through the lower path ($\tilde{n} = n-1$)

In this case, $\hat{C}_{r,+,n-1}^{(1)}$ and $\hat{C}_{\varphi,+,n-1}^{(1)}$ are given by equations (81) and (82). Hence, in the lowest order of approximations we have, from equations (49) and (50),

$$\begin{aligned} \hat{\zeta}_{r,+,n-1}^{(1)} &= -in(kH)\Omega_{\perp}^4 \frac{-\kappa^2 + \tilde{n}\Omega_{\perp}^2}{-\kappa^2 + n\Omega_{\perp}^2} \hat{\xi}_r^{(0)} \\ &\quad \times \left\{ \frac{d\ln\Omega_{\perp}^2}{dr} \eta + \frac{-\kappa^2 + \Omega_{\perp}^2}{\Omega_{\perp}^2} \left[\frac{d\eta}{dr} - \frac{2\Omega}{\omega - (m+1)\Omega} \frac{\eta}{r} \right] \right\}, \end{aligned} \quad (89)$$

$$\hat{\zeta}_{\varphi,+,n-1}^{(1)} = i \frac{2\Omega}{\omega - (m+1)\Omega} \hat{\zeta}_{r,+,n-1}^{(1)}. \quad (90)$$

In deriving \tilde{W} , we do not need $\hat{\zeta}_{z,+,n-1}^{(1)}$.

Using the above expressions, we can obtain $\hat{C}_{+,n-1}^{(2)}$. The results are summarized as

$$\hat{C}_{r,+,n-1}^{(2)} = i(kH)\Omega_{\perp}^2 \hat{\zeta}_{r,+,n-1}^{(1)} \left[\frac{d\eta^*}{dr} - \frac{2\Omega}{\omega - (m+1)\Omega} \frac{\eta^*}{r} \right], \quad (91)$$

$$\hat{C}_{z,+,n-1}^{(2)} = \Omega_{\perp}^2 \hat{\zeta}_{r,+,n-1}^{(1)} \left\{ -\frac{d\ln\Omega_{\perp}^2}{dr} \eta^* + (n-1) \left[\frac{d\eta^*}{dr} - \frac{2\Omega}{\omega - (m+1)\Omega} \frac{\eta^*}{r} \right] \right\}. \quad (92)$$

The φ -component, $\hat{C}_{\varphi,+,n-1}^{(2)}$, is not presented here, since it is smaller than $\hat{C}_{r,+,n-1}^{(2)}$ and does not contribute to \tilde{W} . Taking into account these results, we finally have, after some manipulations,

$$\tilde{W} = n! \xi_{r,+,n-1}^{(0)*} \hat{C}_{r,+,n-1}^{(2)} + (n-1)! \xi_{z,+,n-1}^{(0)*} \hat{C}_{z,+,n-1}^{(2)} = \frac{\tilde{n}!}{-\kappa^2 + \tilde{n}\Omega_{\perp}^2} |\zeta_{r,+,n-1}^{(1)}|^2. \quad (93)$$

7.1.2. Vertical resonances of g -mode oscillations

(a) Coupling through the upper path ($\tilde{n} = n+1$)

Expressions for $\hat{C}_{r,+,n+1}^{(1)}$ and $\hat{C}_{z,+,n+1}^{(1)}$ are the same as those for the horizontal resonances given by equations (79) and (80). In the present case of vertical resonances, however, expressions for the lowest order of approximations of $\hat{\zeta}_{+,n+1}^{(1)}$ are different from those in the horizontal resonances. In the expression for $\hat{\zeta}_{r,+,n}^{(1)}$ [equation (49)], the terms coming from $\hat{C}_{r,+,n+1}^{(1)}$ and $\hat{C}_{\varphi,+,n+1}^{(1)}$ are smaller than the term of $\hat{C}_{z,+,n+1}^{(1)}$, since $[\omega - (m+1)\Omega]^2 - \tilde{n}\Omega_{\perp}^2$ is now small by the resonance being vertical. The results of calculations are

$$\begin{aligned} \hat{\zeta}_{r,+,n+1}^{(1)} &= -i(kH)\Omega_{\perp}^2 \hat{C}_{z,+,n+1}^{(1)} \\ &= -i(kH)\Omega_{\perp}^4 \hat{\xi}_r^{(0)} \left[-\frac{d\ln\Omega_{\perp}^2}{dr} \eta + n \left(\frac{d\eta}{dr} + \frac{2\Omega}{\omega - m\Omega} \frac{\eta}{r} \right) \right], \end{aligned} \quad (94)$$

$$\hat{\zeta}_{z,+,n+1}^{(1)} = i(kH)^{-1} \frac{\kappa^2 - \tilde{n}\Omega_{\perp}^2}{\Omega_{\perp}^2} \hat{\zeta}_{r,+,n+1}^{(1)}, \quad (95)$$

where the expression for $\hat{\zeta}_{\varphi,+,n+1}^{(1)}$ is not presented, since it is the same as equation (84). These equations show that, different from the case of horizontal resonances, the intermediate oscillations have the largest amplitude in the vertical direction.

By using $\hat{\zeta}_{+,n+1}^{(1)}$ given above, we can calculate $\hat{C}_{+,n+1}^{(2)}$. The results show that the main terms of $\hat{C}_{+,n+1}^{(2)}$ are

$$\hat{C}_{r,+,n+1}^{(2)} = \Omega_{\perp}^2 \hat{\zeta}_{z,+,n+1}^{(1)} \left(-\frac{d\ln\Omega_{\perp}^2}{dr} \eta^* + n \frac{d\eta^*}{dr} \right), \quad (96)$$

$$\hat{C}_{\varphi,+,n+1}^{(2)} = in\Omega_{\perp}^2 \hat{\zeta}_{z,+,n+1}^{(1)} \frac{\eta^*}{r}. \quad (97)$$

The z -component, $\hat{C}_{z,+,n+1}^{(2)}$, is found to be unnecessary here. From these results, we finally have

$$\tilde{W} = n! \left[\hat{\xi}_r^{(0)} \hat{C}_{r,+,n+1}^{(2)} + \hat{\xi}_{\varphi}^{(0)} \hat{C}_{\varphi,+,n+1}^{(2)} \right] = -\frac{(\tilde{n}-2)!}{-\kappa^2 + \tilde{n}\Omega_{\perp}^2} |\hat{\zeta}_{z,+,n+1}^{(1)}|^2. \quad (98)$$

(b) Coupling through the lower path ($\tilde{n} = n-1$)

The expressions for $\hat{C}_{r,+,n-1}^{(1)}$ and $\hat{C}_{\varphi,+,n-1}^{(1)}$ are the same as those given by equations (81) and (82), respectively, and $\hat{C}_{z,+,n-1}^{(1)}$ is unnecessary, as in the case of (b) of subsection 7.1.1. Hence, all of the procedures go on in parallel, like in subsection 7.1.1. In subsection

7.1.1. in deriving $\hat{\zeta}_{r,+,n+1}^{(1)}$ from equation (49), $[\omega - (m+1)\Omega]^2 - \tilde{n}\Omega_\perp^2$ was replaced by $\kappa^2 - \tilde{n}\Omega_\perp^2$, since the horizontal resonances are considered there. In the present case of vertical resonances, it can be approximated by $\tilde{n}(kH)^2\Omega_\perp^4/(\tilde{n}\Omega_\perp - \kappa^2)$. Hence, in the present case we have

$$\begin{aligned}\hat{\zeta}_{r,+,n-1}^{(1)} &= -(kH)^2 \frac{\tilde{n}\Omega_\perp^4}{\tilde{n}\Omega_\perp^2 - \kappa^2} \left[\hat{C}_{r,+,n-1}^{(1)} - i \frac{2\Omega}{\omega - (m+1)\Omega} \hat{C}_{\varphi,+,n-1}^{(1)} \right] \\ &= i(kH)^3 \frac{n\tilde{n}\Omega_\perp^8}{(-\kappa^2 + \tilde{n}\Omega_\perp^2)(-\kappa^2 + n\Omega_\perp^2)} \hat{\xi}_r^{(0)} \\ &\quad \times \left\{ \frac{d\ln\Omega_\perp^2}{dr} \eta + \frac{-\kappa^2 + \Omega_\perp^2}{\Omega_\perp^2} \left[\frac{d\eta}{dr} - \frac{2\Omega}{\omega - (m+1)\Omega} \frac{\eta}{r} \right] \right\},\end{aligned}\quad (99)$$

$$\hat{\zeta}_{\varphi,+,n-1}^{(1)} = i \frac{2\Omega}{\omega - (m+1)\Omega} \hat{\zeta}_{r,+,n-1}^{(1)}, \quad (100)$$

$$\hat{\zeta}_{z,+,n-1}^{(1)} = i(kH)^{-1} \frac{n\Omega_\perp^2 - \kappa^2}{\Omega_\perp^2} \hat{\zeta}_{r,+,n-1}^{(1)}. \quad (101)$$

Expressions for $\hat{C}_{r,+,n-1}^{(2)}$ and $\hat{C}_{z,+,n-1}^{(2)}$ are the same as those given by equations (91) and (92). Hence, we finally have

$$\tilde{W} = n! \hat{\xi}_{r,+,n-1}^{(0)} \hat{C}_{r,+,n-1}^{(2)} + (n-1)! \hat{\xi}_{z,+,n-1}^{(0)} \hat{C}_{z,+,n-1}^{(2)} = -\frac{(\tilde{n}-2)!}{-\kappa^2 + \tilde{n}\Omega_\perp^2} |\hat{\zeta}_{z,+,n-1}^{(1)}|^2. \quad (102)$$

7.2. P-Mode Oscillations

In the case of p-mode oscillations, $-(\omega - m\Omega) + n\Omega_\perp^2 \sim 0$, but the dispersion relation shows that it can be approximated as $-n(kH)^2\Omega_\perp^4/(n\Omega_\perp^2 - \kappa^2)$. Hence, from equation (34) we have a relation between $\hat{\xi}_z^{(0)}$ and $\hat{\xi}_r^{(0)}$, which is

$$\hat{\xi}_r^{(0)} = i(kH) \frac{\Omega_\perp^2}{n\Omega_\perp^2 - \kappa^2} \hat{\xi}_z^{(0)}. \quad (103)$$

Furthermore, equation (33) gives

$$\hat{\xi}_\varphi^{(0)} = i \frac{2\Omega}{\omega - m\Omega} \hat{\xi}_r^{(0)}. \quad (104)$$

These relations show that in the p-mode oscillations $\hat{\xi}_z^{(0)}$ is major and that $\hat{\xi}_r^{(0)}$ and $\hat{\xi}_\varphi^{(0)}$ are smaller than $\hat{\xi}_z^{(0)}$ by a factor of kH , as expected.

As mentioned before, we have only horizontal resonances, i.e., the vertical resonances are absent in the case of p-mode oscillations.

7.2.1. Horizontal resonances of p-mode oscillations

As in the case of g-mode oscillations, two coupling paths are treated separately.

(a) Coupling through the upper path ($\tilde{n} = n+1$)

Expressions for $\hat{C}_{r,+,n+1}^{(1)}$ and $\hat{C}_{z,+,n+1}^{(1)}$ are the same as equations (79) and (80), respectively. ($\hat{C}_{\varphi,+,n+1}^{(1)}$ is unnecessary, since it is small.) The expressions for $\hat{\zeta}_{r,+,n+1}^{(1)}$ and $\hat{\zeta}_{z,+,n+1}^{(1)}$ are also the same as those given by equations (83) and (85), respectively. The coupling terms,

$\hat{C}_{r,+,n+1}^{(2)}$ and $\hat{C}_{\varphi,+,n+1}^{(2)}$ are thus the same as those given by equations (86) and (87). The term $\hat{C}_{z,+,n+1}^{(2)}$ is unnecessary, since it is small and does not contribute to the final results.

Using the above results, we finally have

$$\tilde{W} = n! \left[\hat{\xi}_r^{(0)} \hat{C}_{r,+,n+1}^{(2)} + \hat{\xi}_\varphi^{(0)} \hat{C}_{\varphi,+,n+1}^{(2)} \right] = \frac{\tilde{n}!}{-\kappa^2 + \tilde{n}\Omega_\perp^2} |\hat{\zeta}_{r,+,n+1}^{(1)}|^2. \quad (105)$$

This expression for \tilde{W} is the same as equation (88), but its concrete figure is different from that of equation (88), since the expressions for $\hat{\xi}_r^{(0)}$ and $\hat{\xi}_z^{(0)}$ are different from those of the g-mode oscillations (see table 1).

(b) Coupling through the lower path ($\tilde{n} = n - 1$)

The coupling terms in the first stage are found to be

$$\hat{C}_{r,+,n-1}^{(1)} = \Omega_\perp^2 \hat{\xi}_z^{(0)} \left[-\frac{d\ln\Omega_\perp^2}{dr} \eta + \tilde{n} \frac{d\eta}{dr} \right], \quad (106)$$

$$\hat{C}_{\varphi,+,n-1}^{(1)} = -i\tilde{n}\Omega_\perp^2 \hat{\xi}_z^{(0)} \frac{\eta}{r}. \quad (107)$$

These expressions for $\hat{C}_{r,+,n-1}^{(1)}$ and $\hat{C}_{\varphi,+,n-1}^{(1)}$ are different from equations (81) and (82), respectively, since the terms of $\hat{\xi}_r^{(0)}$ can be neglected in the present case.

Using the above expressions, we have

$$\hat{\zeta}_{r,+,n-1}^{(1)} = (-\kappa^2 + \tilde{n}\Omega_\perp^2) \Omega_\perp^2 \hat{\xi}_z^{(0)} \left\{ -\frac{d\ln\Omega_\perp^2}{dr} \eta + \tilde{n} \left[\frac{d\eta}{dr} - \frac{2\Omega}{\omega - (m+1)\Omega} \frac{\eta}{r} \right] \right\}. \quad (108)$$

Expressions for $\hat{\zeta}_{\varphi,+,n-1}^{(1)}$ and $\hat{\zeta}_{z,+,n-1}^{(1)}$ are not shown here, since they are the same as equations (84) and (85), respectively, except for the subscript $n+1$ being replaced by $n-1$. Consequently, as the final results concerning \tilde{W} , we have

$$\tilde{W} = (n-1)! \hat{\xi}_z^{(0)} \hat{C}_{z,+,n-1}^{(2)} = \frac{\tilde{n}!}{-\kappa^2 + \tilde{n}\Omega_\perp^2} |\hat{\zeta}_{r,+,n-1}^{(1)}|^2. \quad (109)$$

So far, we have restricted our attention to the coupling cases of $m \rightarrow m+1 \rightarrow m$. Even in the case of $m \rightarrow m-1 \rightarrow m$, however, the derivation of the \tilde{W} 's is similar. The results show that the final expressions for \tilde{W} 's are the same, except that the subscript $+$ in $\hat{\zeta}_{r,+,n+1}^{(1)}$, $\hat{\zeta}_{r,+,n-1}^{(1)}$, $\hat{\zeta}_{z,+,n+1}^{(1)}$, or $\hat{\zeta}_{z,+,n-1}^{(1)}$ in equations (88), (93), (98), (102), (105), or (109) is replaced by the subscript $-$. The difference between $\hat{\zeta}_{r,+,n+1}^{(1)}$ and $\hat{\zeta}_{r,-,n+1}^{(1)}$, for example, is that $m+1$ in the expressions for $\hat{\zeta}_{r,+,n+1}^{(1)}$ is changed to $m-1$ in $\hat{\zeta}_{r,-,n+1}^{(1)}$.

Next, we summarize the expressions of growth rate. As mentioned in section 5, the sign of $[\omega - (m \pm 1)\Omega]/(\omega - m\Omega)$ is negative in the horizontal resonances of g-mode oscillations. Hence, in this case we have, from equation (73) and expressions for \tilde{W} 's given above,

$$-\omega_i = \frac{\pi/8}{(-\kappa^2 + \tilde{n}\Omega^2)^2} \left| \frac{G_{H,\pm,\tilde{n}}}{\omega - m\Omega} \right|_c \frac{\tilde{n}! |\hat{\zeta}_{r,\pm,\tilde{n}}^{(1)}|_c^2}{\hat{E}}, \quad (110)$$

which is positive, and thus the resonant oscillations are amplified ($-\omega_i > 0$). In the cases of horizontal resonances of p-mode oscillations (excluding $n = 0$), on the other hand, the sign of $[\omega - (m \pm 1)\Omega]/(\omega - m\Omega)$ at the resonant point is positive, and we have

$$-\omega_i = -\frac{\pi/8}{(-\kappa^2 + \tilde{n}\Omega^2)^2} \left| \frac{G_{H,\pm,\tilde{n}}}{\omega - m\Omega} \right|_c \frac{\tilde{n}! |\hat{\zeta}_{r,\pm,\tilde{n}}^{(1)}|_c^2}{\hat{E}}, \quad (111)$$

which is negative and the resonances lead to damping of the oscillations.

In the case of vertical resonances of g-mode oscillations, the situations are a little different. The sign of $[\omega - (m \pm 1)\Omega]/(\omega - m\Omega)$ is positive in this case. In the case of vertical resonances, the sign of $\int (1/D)dr$ is opposite to that in the case of horizontal resonances [see equations (69) and (72)]. The signs of the \hat{W} 's given above are also opposite to those in the case of horizontal resonances. Considering them, we have

$$-\omega_i = -\frac{\pi/8}{(-\kappa^2 + \tilde{n}\Omega^2)^2} \left| \frac{G_{V,\pm,\tilde{n}}}{\omega - m\Omega} \right|_c \frac{(\tilde{n} - 2)! |\hat{\zeta}_{z,\pm,\tilde{n}}^{(1)}|_c^2}{\hat{E}}, \quad (112)$$

and the oscillations are damped.

8. Discussion

In this paper the resonant excitations of disk oscillations on relativistic disks deformed by a warp have been examined, considering non-linear couplings between the oscillations and the warp. The non-linear couplings that we consider are schematically shown in figure 1. The resonant processes involved in the couplings bring about amplification, or damping, of the original disk oscillations. First, a general stability criterion of the resonances is derived by using the Lagrangian formulation developed by Lynden-Bell and Ostriker (1974). Then, the criterion is applied to studying the resonant amplification.

There are three types of resonances: i) horizontal and ii) vertical resonances of g-mode oscillations and iii) vertical resonances of p-mode oscillations. For each case, four coupling paths between the oscillations and the warp are possible, i.e., $m \rightarrow m \pm 1 \rightarrow m$ and $n \rightarrow n \pm 1 \rightarrow n$. Detailed examinations where the resonances occur and how much the frequencies of the resonant oscillations are were made in Paper I. In this paper we thus concentrate on whether these resonances amplify or dampen the oscillations. The results concerning their growth rates are summarized in equations (110)–(112). It should be emphasized that the presence of resonances is completely an effect of general relativity. This is because a difference in the spatial distributions of $\Omega(r)$ and $\kappa(r)$ is essential for the resonances, and it results from the disk being general relativistic.

Although the detailed interaction processes are different in each type of resonances and in each coupling path, the final expressions for \tilde{W} have similar compact forms for all cases [see equations (88), (93), (98), (102), (105), and (109)], which suggests the correctness of our manipulations. [The results of Kato (2003) are not always correct, since there are some errors in the calculations.]

In the case of horizontal resonances, \tilde{W} can be compactly expressed in terms of $\hat{\zeta}_r^{(1)}$, while it is expressed in terms of $\hat{\zeta}_z^{(1)}$ in the case of vertical resonances, as expected. Although

Table 1. Growth rates and resonant radii.

Type of resonance	Path	Growth rate	Radii
g-mode, horizontal	$\tilde{n} = n \pm 1$	$\alpha(kH)^2\Omega$	$\sim 4.0r_g$
g-mode, vertical	$\tilde{n} = n + 1$	$-\alpha\Omega$ (damping)	$\sim 3r_g, 3.62r_g, 6.46r_g$
	$\tilde{n} = n - 1$	$-\alpha(kH)^4\Omega$	$\sim 3r_g, 3.62r_g, 6.46r_g$
p-mode, horizontal ($n \neq 0$)	$\tilde{n} = n + 1$	$-\alpha(kH)^4\Omega$ (damping)	$\sim 3r_g, 3.62r_g, 6.46r_g$
	$\tilde{n} = n - 1$	$-\alpha\Omega$ (damping)	$\sim 3r_g, 3.62r_g, 6.46r_g$

the expressions for \tilde{W} are similar in all cases, concrete figures of the growth rates are different in each case, since the expressions for $\hat{\xi}_r^{(1)}$ (or $\hat{\xi}_z^{(1)}$) are different in each case. Let us now estimate the order of the growth (or damping) rate. The amplitudes of intermediate oscillations, $\hat{\xi}^{(1)}$, are given in section 7 for various types of resonances. Hence, using them we can estimate the order of the growth rates, which are summarized in table 1. In table 1, α denotes $|\eta|_c^2/r_c L$, where L is the radial size of the wave packet of the oscillations, and \hat{E} has been estimated by $\hat{E} \sim |\hat{\xi}_r^{(0)}|^2 L/r$ for g-mode oscillations and by $\hat{E} \sim |\hat{\xi}_z^{(0)}|^2 L/r$ for p-mode oscillations. The radii where the resonances for the oscillations of $k \sim 0$ occur are also given in table 1 (see also Paper I). It is noted that in table 1 p-mode oscillations of $n = 0$ are included in g-mode oscillations.

The radii given in table 1 are those where both curves specifying the propagation region and the resonance region cross on the ω - r plane. In other words, they are radii where long-wavelength oscillations have resonances. We think that long-wavelength oscillations are of interest, since they are most observable (little phase mixing and little group velocity in the radial direction). The growth (or damping) rate of the oscillations, however, tends to zero in the limit of long wavelength of $kH = 0$. Hence, the oscillations that are of interest are those slightly apart from the radii given in the table.

Table 1 shows that the vertical resonances of the g-mode oscillations with $\tilde{n} = n + 1$ and the horizontal resonances of the p-mode oscillations with $\tilde{n} = n - 1$ are strongly damped [see the absence of a small factor of (kH)]. The growing modes are horizontal resonances of the g-mode oscillations alone, including the horizontal resonances of the p-mode oscillations of $n = 0$. The growth rates of these oscillations are on the order of $\alpha\Omega_c$ times $(kH)^2$. This suggests that the quasi-periodic oscillations caused by our present mechanism are observable when the disks are moderately thick.

Let us hereafter focus only on the growing oscillations, which are all amplified around $4.0r_g$. The reason why $4.0r_g$ is the resonance radius is that the resonance condition for horizontal resonances of g-mode oscillations is $2\kappa = \Omega$ (see section 5), and this is realized there in the case of the Schwarzschild metric. The frequencies of the resonant oscillations are $\kappa, \Omega \pm \kappa, 2\Omega \pm \kappa, \dots$ at $r = 4r_g$ (see Paper I), depending on the modes (m and n) of the oscillations. In units of

⁰ α in table 1 denotes $|\eta|_c^2/r_c L$.

$(GM/r_g^3)^{1/2}$, these frequencies are

$$0.0625, \quad 0.1875, \quad 0.313, \quad 0.4375, \quad (113)$$

and their ratios are $1 : 3 : 5 : 7 \dots$. The modes of oscillations realizing these frequencies are summarized in table 2.

If we are concerned with what frequencies are observable in luminosity variations, some other frequencies should be added in the list of equation (113) for the following reason. Let us consider one-armed ($m = 1$) oscillations with frequency ω . Then, a one-armed pattern revolves around the disk center with frequency ω . After half a revolution, however, the arm appears on the another side of the disk. Hence, if we observe luminosity variations (not velocity variations) resulting from the whole disk, the phases of the luminosity variations become the same as the initial one after half a revolution. That is, we observe a luminosity variation with frequency 2ω . As shown in table 2, the oscillations of κ (or $\Omega - \kappa$) are realized by one-armed oscillations. Hence, we can expect luminosity variations with frequency $2\kappa (= \Omega)$. A similar argument shows that we can also expect a luminosity variation of $2(\Omega + \kappa)$ or $2(2\Omega - \kappa)$, which is 6κ , since oscillations with $\Omega + \kappa$ or $2\Omega - \kappa$ occur for one-armed oscillations. The above argument, however, cannot be applied to $m = 2$ oscillations. One-armed oscillations have a unique characteristic in this sense. Summing them, we can say that the observed frequencies are some hamonics of κ , as follows:

$$0.0625, \quad 0.125, \quad 0.1875, \quad 0.313, \dots \quad (114)$$

in the case of the Schwarzschild metric. Their ratios are $1 : 2 : 3 : 5 : 6 : 7 \dots$

The lowest frequency of oscillations, κ , is hidden by the oscillations of 2κ . The most observable pairs of oscillations are thus $2 : 3$. This will be the reason why $2 : 3$ oscillations are prominently observed as QPOs in black hole candidates. The above arguments suggest that other sets of oscillations, for example, $1 : 2$ and $3 : 5$, are also observable candidates. It is noted that the importance of $2 : 3$ pair oscillations was first emphasized by Abramowicz and Kluźniak (2001) and Kluźniak and Abramowicz (2001), although they did not present definite resonant mechanisms.

Next, we estimate the masses (and spins) of four black-hole objects with pairs of QPOs. In all of them, the pairs are close to $2 : 3$. If we take the observed upper frequencies of these QPOs to be $3\kappa(r_{\max})$ with the Schwarzschild metric, the masses of the central black hole can be calculated for each object. The results are shown on the fourth line of table 3. The second line of table 3 shows the observed pairs of frequencies in units of hertz, and the bottom line of the table shows the mass ranges (in units of the solar mass) which were evaluated from the observed data. In XTE 1550–564 and GRO 1655–40, the masses estimated by our model are slightly below the mass ranges obtained from observations. One of the reasons would be that effects of the rotation of the central objects are not taken into account in evaluating the frequencies.

Table 2. Frequencies and modes of resonant oscillations.

Frequencies		Modes of oscillations	
	in units of $(GM/r_g^3)^{1/2}$	g-mode (arbitrary n)	p-mode ($n = 0$)
$\kappa, \Omega - \kappa$	0.0625	$m = 0, 1$	$m = 0, 1$
$\Omega + \kappa, 2\Omega - \kappa$	0.1875	$m = 1, 2$	$m = 1, 2$
$2\Omega + \kappa, 3\Omega - \kappa$	0.313	$m = 2, 3$	$m = 2, 3$

Table 3. Estimated masses of four black hole candidates.

Objects	GRS 1915+105 ^(*)		XTE 1550–564 ^(*)	GRO 1655–40 ^(*)	H 1743–322 ⁽⁺⁾
Frequencies	(113, 168)		(184, 276)	(300, 450)	(160, 240)
a	r_c/r_g	M/M_\odot	M/M_\odot	M/M_\odot	M/M_\odot
0.0	4.0	12.6	8.19	4.75	8.90
0.1	3.84	13.4	8.78	5.04	9.44
0.2	3.66	14.3	9.26	5.37	10.1
0.3	3.48	15.3	9.93	5.76	10.8
0.4	3.29	16.5	10.7	6.22	11.7
0.5	3.08	18.0	11.7	6.79	12.7
		10.0 – 18.0	8.4 – 10.8	6.0 – 6.6	not measured

The processes for deriving the resonance condition $2\kappa = \Omega$ in this paper suggest that even when the central object has rotation, the condition for horizontal resonances of g-mode oscillations remains $2\kappa = \Omega$ in the lowest order of approximations. Using the Kerr metric with the spin parameter a ($0 \leq a < 1$), we can calculate, as a function of a , the radius where $2\kappa = \Omega$ is realized. Then, κ (or Ω) values at the radius are obtained as functions of the mass and spin of the central objects. Comparing the frequencies calculated in this way with observations, we can estimate the masses of the central objects as a function of a . The results are also presented in table 3, which shows that the masses evaluated by our model are in good agreement with observations for moderate values of a . Let us denote the upper frequency of the twin pairs by ν_{upp} . Then, the relation between ν_{upp} and the mass, M , for a given a is

$$\nu_{\text{upp}} = A \left(\frac{M}{M_\odot} \right)^{-1} \text{ kHz}, \quad (115)$$

where $A = 2.1, 2.4, 2.8$, and 3.4 for $a = 0, 0.2, 0.4$, and 0.6 , respectively. The relation in the case of $a = 0.4$ is just the same as that obtained by McClintock and Remillard (2003) as a fitting formula of observations.

The frequency ratios of some observed QPO pairs are slightly deviated from $2 : 3$. This occurs naturally in our model, since oscillations propagate in the radial direction as a wave

⁰ (*) McClintock & Remillard (2003), (+) Homan et al. (2003). See also Abramowicz et al. (2004b).

packet, changing the resonant frequencies and their wavelengths. Another possibility of the deviation is precession of the warp. A precession of the warp is generally expected when the central object has rotation. If this interpretation is correct, the frequency of the precession is related to the deviation, and the precession might be observed as a low-frequency QPO. Large Q -values of QPOs are also expected in our model, since the oscillations are not trapped standing ones. Furthermore, different modes of oscillations with different paths of couplings appear with close frequencies, as shown in table 2 (see also Paper I).

If our present model represents the real mechanism of kHz QPOs, observations of QPOs are a powerful tool for evaluating the mass and spin of the central black holes. Furthermore, it is implied that a warp occasionally appears in the innermost region of relativistic disks. This would be of importance for understanding the activities, structures, and evolutions of the innermost region of black-hole disks.

Finally, it is noted that the basic process of our resonance model is applicable to any deformed disks. For example, if the disks are deformed by the spin of the central objects through a spin-disk coupling, we can expect disk oscillations whose frequencies are correlated to the spin frequency. It is known that in some X-ray binaries with neutron stars, the frequency difference between the high frequency QPO pairs is equal to, or half of, the spin frequency (Wijnands et al. 2003). In a subsequent paper we will examine whether the phenomenon could be explained by a simple extension of our present resonance model.

Appendix 1. Expressions for C in Cylindrical Coordinates

The coupling term $C(\xi, \xi)$ consists of two terms as $C = C_\psi + C_p$. Expressions for C_ψ and C_p in cylindrical coordinates are

$$\rho_0 C_{\psi,r} = -\frac{1}{2}\rho_0 \left[\left(\xi_r^2 \frac{\partial^2}{\partial r^2} + 2\xi_r \xi_z \frac{\partial^2}{\partial r \partial z} + \xi_z^2 \frac{\partial^2}{\partial z^2} \right) \frac{\partial \psi_0}{\partial r} - \frac{\xi_\varphi^2}{r^2} \frac{\partial \psi_0}{\partial r} + \frac{\xi_\varphi^2}{r} \frac{\partial^2 \psi_0}{\partial r^2} \right], \quad (116)$$

$$\rho_0 C_{\psi,\varphi} = -\rho_0 \left[\xi_r \xi_\varphi \frac{\partial}{\partial r} \left(\frac{1}{r} \frac{\partial \psi_0}{\partial r} \right) + \frac{\xi_\varphi \xi_z}{r} \frac{\partial^2 \psi_0}{\partial r \partial z} \right], \quad (117)$$

$$\rho_0 C_{\psi,z} = -\frac{1}{2}\rho_0 \left[\left(\xi_r^2 \frac{\partial^2}{\partial r^2} + 2\xi_r \xi_z \frac{\partial^2}{\partial r \partial z} + \xi_z^2 \frac{\partial^2}{\partial z^2} \right) \frac{\partial \psi_0}{\partial z} + \frac{1}{r} \xi_\varphi^2 \frac{\partial^2 \psi_0}{\partial r \partial z} \right], \quad (118)$$

$$\rho_0 C_{p,r} = -\frac{\partial T_{rr}}{\partial r} - \frac{\partial T_{\varphi r}}{r \partial \varphi} - \frac{\partial T_{zr}}{\partial z} - \frac{1}{r} T_{rr} + \frac{1}{r} T_{\varphi \varphi}, \quad (119)$$

$$\rho_0 C_{p,\varphi} = -\frac{\partial T_{r\varphi}}{\partial r} - \frac{\partial T_{\varphi\varphi}}{r \partial \varphi} - \frac{\partial T_{z\varphi}}{\partial z} - \frac{1}{r} (T_{r\varphi} + T_{\varphi r}), \quad (120)$$

$$\rho_0 C_{p,z} = -\frac{\partial T_{rz}}{\partial r} - \frac{\partial T_{\varphi z}}{r \partial \varphi} - \frac{\partial T_{zz}}{\partial z} - \frac{1}{r} T_{rz}, \quad (121)$$

where

$$T_{rr} = p_0 \left[\left(\frac{\partial \xi_r}{\partial r} \right)^2 + \left(\frac{\partial \xi_r}{r \partial \varphi} - \frac{\xi_\varphi}{r} \right) \frac{\partial \xi_\varphi}{\partial r} + \frac{\partial \xi_r}{\partial z} \frac{\partial \xi_z}{\partial r} \right], \quad (122)$$

$$T_{r\varphi} = p_0 \left[\left(\frac{\partial \xi_r}{\partial r} + \frac{\partial \xi_\varphi}{r \partial \varphi} + \frac{\xi_r}{r} \right) \left(\frac{\partial \xi_r}{r \partial \varphi} - \frac{\xi_\varphi}{r} \right) + \frac{\partial \xi_r}{\partial z} \frac{\partial \xi_z}{r \partial \varphi} \right], \quad (123)$$

$$T_{rz} = p_0 \left[\frac{\partial \xi_r}{\partial r} \frac{\partial \xi_r}{\partial z} + \left(\frac{\partial \xi_r}{r \partial \varphi} - \frac{\xi_\varphi}{r} \right) \frac{\partial \xi_\varphi}{\partial z} + \frac{\partial \xi_r}{\partial z} \frac{\partial \xi_z}{\partial z} \right], \quad (124)$$

$$T_{\varphi r} = p_0 \left[\frac{\partial \xi_\varphi}{\partial r} \frac{\partial \xi_r}{\partial r} + \left(\frac{\partial \xi_\varphi}{r \partial \varphi} + \frac{\xi_r}{r} \right) \frac{\partial \xi_\varphi}{\partial r} + \frac{\partial \xi_\varphi}{\partial z} \frac{\partial \xi_z}{\partial r} \right], \quad (125)$$

$$T_{\varphi\varphi} = p_0 \left[\frac{\partial \xi_\varphi}{\partial r} \left(\frac{\partial \xi_r}{r \partial \varphi} - \frac{\xi_\varphi}{r} \right) + \left(\frac{\partial \xi_\varphi}{r \partial \varphi} + \frac{\xi_r}{r} \right)^2 + \frac{\partial \xi_\varphi}{\partial z} \frac{\partial \xi_z}{r \partial \varphi} \right], \quad (126)$$

$$T_{\varphi z} = p_0 \left[\frac{\partial \xi_\varphi}{\partial r} \frac{\partial \xi_r}{\partial z} + \left(\frac{\partial \xi_\varphi}{r \partial \varphi} + \frac{\xi_r}{r} \right) \frac{\partial \xi_\varphi}{\partial z} + \frac{\partial \xi_\varphi}{\partial z} \frac{\partial \xi_z}{\partial z} \right], \quad (127)$$

$$T_{zr} = p_0 \left[\frac{\partial \xi_z}{\partial r} \frac{\partial \xi_r}{\partial r} + \frac{\partial \xi_z}{r \partial \varphi} \frac{\partial \xi_\varphi}{\partial r} + \frac{\partial \xi_z}{\partial z} \frac{\partial \xi_z}{\partial r} \right], \quad (128)$$

$$T_{zz} = p_0 \left[\frac{\partial \xi_z}{\partial r} \left(\frac{\partial \xi_r}{r \partial \varphi} - \frac{\xi_\varphi}{r} \right) + \frac{\partial \xi_z}{r \partial \varphi} \left(\frac{\partial \xi_\varphi}{r \partial \varphi} + \frac{\xi_r}{r} \right) + \frac{\partial \xi_z}{\partial z} \frac{\partial \xi_z}{r \partial \varphi} \right], \quad (129)$$

and

$$T_{zz} = p_0 \left[\frac{\partial \xi_z}{\partial r} \frac{\partial \xi_r}{\partial z} + \frac{\partial \xi_z}{r \partial \varphi} \frac{\partial \xi_\varphi}{\partial z} + \frac{\partial \xi_z}{\partial z} \frac{\partial \xi_z}{\partial z} \right]. \quad (130)$$

Appendix 2. Expressions for $\hat{C}_{r,\pm,\tilde{n}}^{(1)}$, $\hat{C}_{\varphi,\pm,\tilde{n}}^{(1)}$, and $\hat{C}_{z,\pm,\tilde{n}}^{(1)}$

From the expressions in appendix 1, we have

$$\begin{aligned} \hat{C}_{r,+,n+1}^{(1)} = & \Omega_\perp^2 H \left\{ -\frac{1}{\Omega_\perp^2} \frac{d^2 \Omega_\perp^2}{dr^2} \hat{\xi}_r \eta \right. \\ & \left. + \frac{d\hat{\xi}_r}{dr} \frac{d\eta}{dr} - i \frac{d\hat{\xi}_\varphi}{dr} \frac{\eta}{r} + n \frac{d \ln H}{dr} \left[-2\hat{\xi}_r \frac{d\eta}{dr} + i\hat{\xi}_\varphi \frac{\eta}{r} \right] \right\}, \end{aligned} \quad (131)$$

$$\begin{aligned} \hat{C}_{r,+,n-1}^{(1)} = & \Omega_\perp^2 H \left\{ -n \frac{1}{\Omega_\perp^2} \frac{d^2 \Omega_\perp^2}{dr^2} \hat{\xi}_r \eta - \frac{d \ln \Omega_\perp^2}{dr} \frac{\hat{\xi}_z}{H} \eta - \frac{n}{r p_{00} H} \frac{d}{dr} \left(r p_{00} \hat{\xi}_r \frac{d\eta}{dr} \right) \right. \\ & \left. + n(n-1) \frac{d \ln H}{dr} \left[-2\hat{\xi}_r \frac{d\eta}{dr} + i\hat{\xi}_\varphi \frac{\eta}{r} \right] + i n \frac{\hat{\xi}_\varphi}{r} \left[(m+1) \frac{d\eta}{dr} - \frac{\eta}{r} \right] + (n-1) \frac{\hat{\xi}_z}{H} \frac{d\eta}{dr} \right\}, \end{aligned} \quad (132)$$

$$\begin{aligned} \hat{C}_{\varphi,+,n+1}^{(1)} = & \Omega_\perp^2 H \left\{ -\frac{d \ln \Omega_\perp^2}{dr} \hat{\xi}_\varphi \frac{\eta}{r} \right. \\ & \left. - (i m \hat{\xi}_r + \hat{\xi}_\varphi) \frac{d\eta}{r dr} - (m \hat{\xi}_\varphi + i \hat{\xi}_r) \frac{\eta}{r^2} + i n \frac{d \ln H}{dr} \hat{\xi}_r \frac{\eta}{r} \right\}, \end{aligned} \quad (133)$$

$$\begin{aligned} \hat{C}_{\varphi,+,n-1}^{(1)} = & \Omega_\perp^2 H \left\{ -n \frac{d \ln \Omega_\perp^2}{dr} \hat{\xi}_\varphi \frac{\eta}{r} + i \frac{n}{p_{00} H^{n-1}} \frac{d}{dr} \left(p_{00} H^{n-1} \hat{\xi}_r \eta \right) \right. \\ & \left. + \frac{n}{r} \left[(m+1) \hat{\xi}_\varphi \frac{\eta}{r} - \hat{\xi}_\varphi \frac{d\eta}{dr} \right] - i(n-1) \frac{\hat{\xi}_z}{H} \frac{\eta}{r} \right\}, \end{aligned} \quad (134)$$

$$\hat{C}_{z,+,n+1}^{(1)} = \Omega_\perp^2 \left\{ -\frac{d \ln \Omega_\perp^2}{dr} \hat{\xi}_r \eta + 9 \frac{H}{r^2} \hat{\xi}_z \eta + n \left(\hat{\xi}_r \frac{d\eta}{dr} - i \hat{\xi}_\varphi \frac{\eta}{r} \right) \right\}, \quad (135)$$

$$\hat{C}_{z,+,n-1}^{(1)} = 3(n-1)\Omega_{\perp}^2 \frac{H^2}{r} \left\{ 3 \frac{\hat{\xi}_z}{H} \frac{\eta}{r} + n \left(\frac{d \ln \Omega_{\perp}^2}{dr} - 2 \frac{\Omega_{\perp}^2}{r} \right) \hat{\xi}_r \frac{\eta}{r} \right\}. \quad (136)$$

The above expressions for the \hat{C} 's are those for the path of $m \rightarrow m+1 \rightarrow m$ (notice $+$ in the subscript). The expressions for the \hat{C} 's resulting from the path of $m \rightarrow m-1 \rightarrow m$ (i.e, \hat{C} 's with the subscript of $-$) are similar to those with a $+$ sign. That is, expressions for \hat{C} 's with the $-$ sign are obtained by changing i and m in the expressions for \hat{C} 's with the $+$ sign to $-i$ and $-m$, respectively. Furthermore, η is changed to η^* .

Appendix 3. Expressions for $\hat{C}_{r,\pm,\tilde{n}}^{(2)}$, $\hat{C}_{\varphi,\pm,\tilde{n}}^{(2)}$, and $\hat{C}_{z,\pm,\tilde{n}}^{(2)}$

Expressions for $\hat{C}_{r,\pm,\tilde{n}}^{(2)}$ can be derived from \mathbf{C} 's given in appendix 1 by similar procedures as in appendix 2. The results of manipulations show that $\hat{C}_{r,+,n+1}^{(2)}(\boldsymbol{\zeta}_{+,n+1}^{(1)}, \boldsymbol{\eta}^*)$ is related to $\hat{C}_{r,-,n-1}^{(1)}(\boldsymbol{\xi}_{-,n-1}^{(0)}, \boldsymbol{\eta}^*)$. That is, the former expression is obtained from the latter one by changing the argument, $\boldsymbol{\xi}_{-,n-1}^{(0)}$, in the latter to $\boldsymbol{\zeta}_{+,n+1}^{(1)}$ and further m and n in the latter, respectively, to $m+1$ and $n+1$. Similarly, $\hat{C}_{r,+,n-1}^{(2)}(\boldsymbol{\zeta}_{+,n-1}^{(1)}, \boldsymbol{\eta}^*)$ is obtained from $\hat{C}_{r,-,n+1}^{(1)}(\boldsymbol{\xi}_{-,n+1}^{(0)}, \boldsymbol{\eta}^*)$ by changing $\boldsymbol{\xi}_{-,n+1}^{(0)}$ in the latter to $\boldsymbol{\zeta}_{+,n-1}^{(1)}$, and m and n to $m+1$ and $n-1$, respectively.

The expression for $\hat{C}_{r,-,n+1}^{(2)}(\boldsymbol{\zeta}_{-,n+1}^{(1)}, \boldsymbol{\eta})$ is obtained from $\hat{C}_{r,+,n-1}^{(1)}(\boldsymbol{\xi}_{+,n-1}^{(0)}, \boldsymbol{\eta})$ by changing $\boldsymbol{\xi}_{+,n-1}^{(0)}$ to $\boldsymbol{\zeta}_{-,n+1}^{(1)}$ and m and n to $m-1$ and $n+1$, respectively. Similarly, $\hat{C}_{r,-,n-1}^{(2)}(\boldsymbol{\zeta}_{-,n-1}^{(1)}, \boldsymbol{\eta})$ is obtained from $\hat{C}_{r,+,n+1}^{(1)}(\boldsymbol{\xi}_{+,n+1}^{(0)}, \boldsymbol{\eta})$ by changing $\boldsymbol{\xi}_{+,n+1}^{(0)}$ to $\boldsymbol{\zeta}_{-,n-1}^{(1)}$ and m and n , respectively, to $m-1$ and $n-1$.

Expressions for $\hat{C}_{\varphi,\pm,\tilde{n}}^{(2)}$ and $\hat{C}_{z,\pm,\tilde{n}}^{(2)}$ are neglected here, since they are easily supposed from the above procedures.

References

- Abramowicz, M. A. & Kluźniak, W. 2001, *A&A*, 374, L19
- Abramowicz, M. A., & Kluźniak, W. 2003, *astro-ph/0312396*
- Abramowicz, M. A., Kluźniak, W., McClintock, J. E., & Remillard, R. A. 2004a, *astro-ph/0402012*
- Abramowicz, M. A., Kluźniak, W., Stuchlik, Z., & Török, G. 2004b, *astro-ph/0401464*
- Hirose, M., & Osaki, Y. 1990, *PASJ*, 42, 135
- Homan, J., Miller, J. M., Wijnands, R., Steeghs, D., Belloni, T., van der Klis, M., & Lewin, W. H. G. 2003, *Atel 162* (<http://integral.rssi.ru/atelmirror>)
- Kato, S. 2001, *PASJ*, 53, 1
- Kato, S. 2003, *PASJ*, 55, 801
- Kato, S. 2004, *PASJ*, 56, 559 (Paper I)
- Kato, S., Fukue, J., & Mineshige, S. 1998, *Black-Hole Accretion Disks* (Kyoto: Kyoto Univ. Press)
- Kato, S., & Tosa, M. 1994, *PASJ*, 46, 559
- Kato, S., & Unno, W. 1967, *PASJ*, 19, 1
- Kluźniak, W., & Abramowicz, M.A. 2001, *Acta Phys. Pol. B32*, 3605
- Lubow, S. H. 1991, *ApJ*, 381, 259
- Lynden-Bell, D., & Ostriker, J. P. 1967, *MNRAS*, 136, 293
- McClintock, J. E., & Remillard, R. A. 2003, *astro-ph/0306213*
- Okazaki, A. T., Kato, S., & Fukue, J. 1987, *PASJ*, 39, 457
- Paczyński, B., & Wiita, P. J. 1980, *A&A*, 88, 23
- Tosa, M. 1994, *ApJ*, 426, L81
- van der Klis, M. 2000, *Ann. Rev. Astron. Astrophys.* 38, 717
- Whitehurst, R. 1988, *MNRAS*, 232, 35
- Wijnands, R., van der Klis, M., Homan, J., Chakrabarty, D., Markwardt, C. B., & Morgan, E. H. 2003, *Nature*, 424, 44